

1 **Comparative analysis of a new assessment of the seismic risk of residential buildings of**
2 **two districts of Barcelona**

3 Armando Aguilar-Meléndez* (ORCID: 0000-0001-9044-7786)^{1 2}, Lluís G. Pujades (0000-0002-2619-
4 0805)³, Alex H. Barbat (0000-0002-3649-8053)³, Marisol Monterrubio-Velasco (0000-0003-0790-1832)²,
5 Josep de la Puente (0000-0003-2608-1526)², Nieves Lantada (0000-0002-9974-6915)³

6 *Correspondence:
7 Armando Aguilar-Meléndez
8 aguilar.uv2@gmail.com

9
10 **Abstract**

11 There are personal and institutional decisions that can increase the seismic resilience of the
12 buildings in a city. However, some of these decisions are possible if we have basic knowledge of
13 buildings' seismic risk. The present document describes the main results of a detailed study of
14 seismic vulnerability and seismic risk of residential buildings of Ciutat Vella (the ancient district of
15 Barcelona) and Nou Barris (one of the newest districts of Barcelona). In this study, we assessed
16 seismic risk according to the Vulnerability Index Method-Probabilistic named as VIM_P. Moreover,
17 we analyzed the influence of basic buildings' features in the final vulnerability and seismic risk
18 values. For instance, we assessed the seismic vulnerability and the seismic risk of groups of buildings
19 defined according to the number of stories of the buildings. Findings of this research reveal that the
20 annual frequency of exceedance of the collapse damage state in Ciutat Vella buildings is, on average,
21 4.7 times higher than for the buildings in Nou Barris. Moreover, according to the *Best* vulnerability
22 curve, 70.31% and 2.81% of Ciutat Vella and Nou Barris buildings, respectively, have an annual
23 frequency of exceedance of the collapse damage state greater than 1×10^{-5} .

24 **Keywords**

25 Seismic risk, Seismic vulnerability, Seismic vulnerability functions, Barcelona
26
27

28 **1. Introduction**
29

30 The seismic risk knowledge is essential information to take actions that can contribute to increasing
31 the seismic resilience in cities. Therefore, each town has the responsibility of assessing its own
32 seismic risk (UNISDR, 2015). Barcelona is a city where the seismic risk is regularly assessed (Aguilar-
33 Meléndez et al. 2019a, b, 2010; Aguilar-Meléndez 2011; Barbat et al. 1996, 2006, 2008, 2009;
34 Carreño et al. 2007; Irizarry et al. 2011; Lantada 2007; Lantada et al. 2009, 2010, 2018; Pujades et

¹ Facultad de Ingeniería Civil, Universidad Veracruzana, Poza Rica, Veracruz, 93390, México.

² Barcelona Supercomputing Center, Plaça Eusebi Güell, 1-3, 08034, Barcelona, Spain.

³ Department of Civil and Environmental Engineering, Universitat Politècnica de Catalunya (UPC),
BarcelonaTech, Barcelona, Spain

35 al. 2000, 2007). Table 1 shows information on relevant examples of the previous studies about
 36 Barcelona’s seismic risk.

37 The present study complements the previous work of Aguilar-Meléndez et al. (2019a,b). In this case,
 38 a new assessment of Barcelona’s seismic hazard was done, applying new ground-motion prediction
 39 equations. The new seismic hazard results were applied to assess the seismic risk of dwelling
 40 buildings of two districts of the city of Barcelona: Ciutat Vella and Nou Barris (Figure 1). Additionally,
 41 a new and detailed comparison between the residential buildings of both districts was performed.
 42 To underline some features of the city of Barcelona, we mention that it has 1664182 inhabitants
 43 (idescat, 2021a). However, in Ciutat Vella and Nou Barris live 6.48% and 10.45%, respectively, of
 44 Barcelona’s mentioned total number of inhabitants (idescat, 2021b).

45 *Table 1. Examples of seismic risk results of Barcelona.*

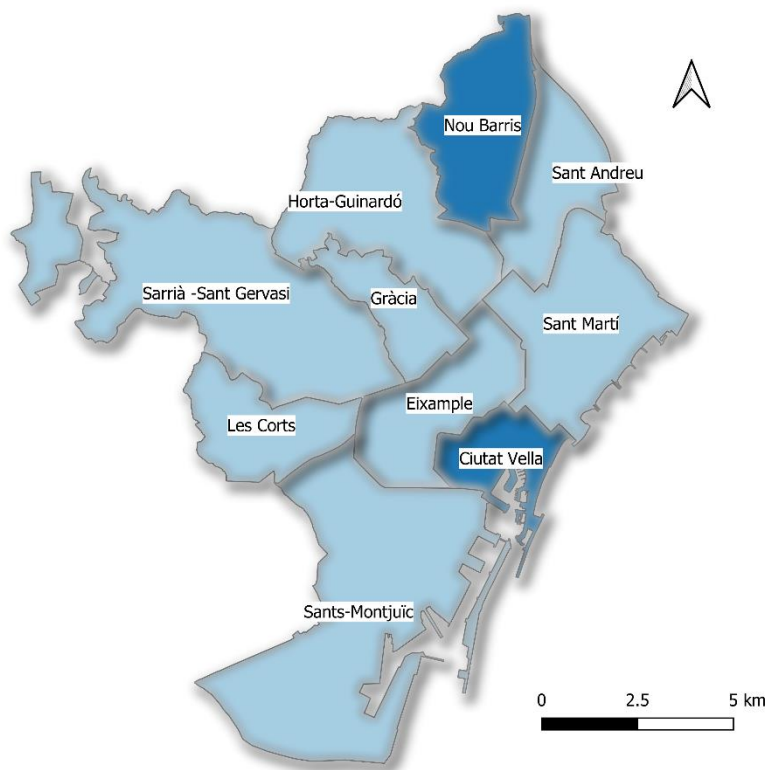
Reference of the study	Method to assess seismic risk	Studied buildings	Seismic hazard considered	Seismic vulnerability results	Seismic risk results
Lantada et al. (2010)	VIM (Risk-UE)	Residential and monumental buildings	Two seismic scenarios: i) a deterministic scenario; ii) a probabilistic scenario for a return period of 475 years.	Census zones classified according to the mean vulnerability index from the residential buildings.	Maps of mean damage grade for each district of Barcelona. Five no null damage grades were considered. Economic losses due to seismic scenarios.
Lantada et al. (2018)	VIM	Residential buildings	Seismic hazard scenarios (V-VI, VI, VI-VII, and VII). The intensity of VI-VII in rock has a 475-year return period.	Average vulnerability index for groups of buildings.	Seismic risk scenarios
Aguilar-Meléndez et al. (2019a,b)	VIM_P	Residential buildings	Probabilistic seismic hazard curve determined by a PSHA.	Vulnerability functions of the buildings.	Annual frequency of exceedance of five damage grades for the city and districts. Seismic risk maps to plot scale for the Eixample district. Economic losses for the city.

46
 47 To assess seismic risk, we applied the Vulnerability Index Method-Probabilistic (VIM_P) proposed
 48 by Aguilar-Meléndez et al. (2019a), which is considered as a complementary method to the
 49 Vulnerability Index Method (VIM) (Milutinovic and Trendafilosky 2003; Lantada et al. 2010). Both
 50 methods (VIM and VIM_P) are based on the assessment of three essential components: 1) seismic
 51 hazard, 2) seismic vulnerability, and 3) seismic risk. However, there are significant differences in the
 52 procedures to assess each one of these components (Milutinovic and Trendafilosky 2003; Aguilar-
 53 Meléndez et al. 2019a).

54 In the VIM, the seismic hazard is considered through seismic scenarios in macroseismic intensities.
 55 Meanwhile, a vulnerability index (a value between zero and one) characterizes the seismic
 56 vulnerability of each examined building. Zero represents low vulnerability and one high vulnerability
 57 (Giovinazzi, 2005; Lantada et al. 2009, 2010). Finally, to compute a mean damage grade (seismic
 58 risk), an empirical function that relates the macroseismic intensity (seismic hazard) and the

59 vulnerability index (seismic vulnerability) is used. The VIM was recently applied to determine the
60 seismic risk of diverse urban areas (Ademović et al. 2020; Cherif et al. 2016; Lestuzzi et al. 2016;
61 Athmani et al. 2015; Guardiola-Víllora and Basset-Salom 2015, 2020; Ruiz et al. 2015). In Spain, the
62 VIM has been applied in two cities: Barcelona (Lantada et al. 2010, 2018) and Valencia (Guardiola-
63 Víllora and Basset-Salom 2015, 2020). It is convenient to highlight that both towns are divided into
64 districts. Simultaneously, they have coincidences on the names of some districts. For instance, in
65 both cities, there is a district called Ciutat Vella, and in both cases, this district is the oldest district
66 of the city. In the present article, all the forthcoming mentions of the Ciutat Vella district correspond
67 to the district with this name in Barcelona.

68 It is appropriate to emphasize that the VIM_P is a procedure that allows incorporating significant
69 uncertainties that the VIM does not consider. Essentially, these uncertainties are incorporated into
70 the seismic vulnerability assessment, which affects the seismic risk results. Additionally, the VIM_P
71 allows obtaining seismic risk in terms of an annual rate of exceedance of both physical damage and
72 loss (Aguilar-Meléndez et al. 2019a).



73
74 *Figure 1. Districts of the city of Barcelona.*

75 At this point, it is useful to mention that the present study has significant differences from the
76 previous works of Aguilar-Melendez et al. (2019a, b). For instance, a relevant difference is the fact
77 that in this study, new seismic hazard curves were determined for Barcelona, and these new curves
78 were used to determine the seismic risk of the residential buildings of Ciutat Vella and Nou Barris.
79 Additionally, in this study, we included a detailed comparison between the results of vulnerability
80 and risk of both districts' buildings.

81 We divided this article into three sections. The first one is the introduction; the second section
82 describes the use of VIM_P to determine the seismic risk of the residential buildings of Ciutat Vella
83 and Nou Barris. This section includes a summary of the VIM_P methodology, information about the
84 data and procedure applied to compute seismic hazard, and a description of the main steps
85 performed to determine vulnerability and seismic risk. Finally, section 3 is devoted to the discussion
86 and conclusions.

87 2. Seismic risk assessment of the residential buildings of Ciutat Vella and Nou Barris

88 2.1. Methodology

89 According to the VIM_P, the three main steps to compute seismic risk are the following: a)
90 probabilistic seismic hazard assessment (PSHA), b) determination of the seismic vulnerability of
91 buildings and c) computation of the seismic risk of buildings under study. In the following sub-
92 sections, we described the main phases that we performed to apply the VIM_P.

93 2.1.1. Seismic hazard in the VIM_P

94 One of the requirements of the VIM_P is that the seismic hazard data to compute seismic risk must
95 be in terms of frequencies of exceedance of macroseismic intensities. Specifically, it is suggested to
96 perform a PSHA to obtain the seismic hazard curve required by the VIM_P (Aguilar-Meléndez et al.
97 2019a). For this last purpose, it is possible to apply validated software as R-CRISIS (Ordaz et al. 2020)
98 or even a previous version of this software as CRISIS2015 (Ordaz et al. 2015; Aguilar-Meléndez et al.
99 2017). It is essential to underline that CRISIS2015 and R-CRISIS allow performing PSHA using
100 accelerations or macroseismic intensities (Ordaz et al. 2020).

101 2.1.2. Seismic vulnerability in the VIM_P

102 According to the VIM_P, the building's seismic vulnerability is computed based on information about
103 the building's main features. This vulnerability is represented by three Beta-type *pdf* functions
104 named *Lower*, *Best*, and *Upper*. The procedure to determine the vulnerability functions was
105 described by Aguilar-Meléndez et al. (2019a). The *Best* vulnerability function represents the main
106 vulnerability of a building. We called it the main vulnerability to highlight that between the three
107 vulnerability curves used in the VIM_P to describe the vulnerability of a building, the best
108 vulnerability curve describes the mean vulnerability and, therefore, the essential vulnerability of the
109 building. In other words, in the VIM_P, the vulnerability of a building must be represented at least
110 by the *Best* vulnerability function. The *Best* vulnerability function is computed applying the following
111 four steps (Aguilar-Meléndez et al. 2019a):

112 i. Estimation of the mean vulnerability index \overline{V}_I .

113 \overline{V}_I is computed according to Eq. (1)

$$\overline{V}_I = V_I^* + \Delta V_R + \Delta V_m \quad (1)$$

114 where V_I^* = vulnerability index of the structural typology; ΔV_R =building regional modifiers; ΔV_m =
115 building-specific modifiers (Milutinovic and Trendafiloski 2003; Lantada 2007). In the case of
116 Barcelona's buildings, the V_I^* values were taken from the building typology matrix (BTM) defined by
117 Milutinovic and Trendafiloski (2003). Additionally, Table 2 shows an example of a V_I^* value.
118 Moreover, the values of ΔV_R and ΔV_m for the buildings of Barcelona were obtained from Lantada
119 (2007).

120 According to the VIM_P, the value of \overline{V}_I will be the mean of the *Best* vulnerability function. This
 121 function will describe the main seismic vulnerability of the studied building.

122

123 *Table 2. Example of vulnerability indices for the typology M34- Unreinforced masonry bearing walls with a floor system*
 124 *based on slabs of reinforced concrete. These indices were obtained from the Risk-UE building typology matrix (BTM)*
 125 *(Milutinovic and Trendafiloski 2003).*

Representative values of the vulnerability ¹				
V_I^{min}	V_I^-	V_I^*	V_I^+	V_I^{max}
0.300	0.490	0.616	0.793	0.860

126 ¹ V_I^* = the value of the vulnerability index (V) that is the most probable. V_I^- and V_I^+ = lower and upper values of the range
 127 of the probable values of V , respectively. V_I^{min} and V_I^{max} = lower and upper values of the range of less probable values of
 128 V , respectively.

129

130 ii. Assessment of the confidence interval (V_c and V_d)

131 V_c and V_d determine the range of the *Best* vulnerability function that contains 90% of the possible
 132 values of V . There are two criteria to compute V_c and V_d (see Eq. 3 and the explanation of Eq.3 in
 133 step iv. See also a detailed description in Aguilar-Mélendez et al. 2019a). In this work, we applied
 134 the simplified criterion that assumes that V_I^{min} and V_I^{max} (Table 2) correspond to V_c and V_d ,
 135 respectively. Therefore in this study, the values of V_c and V_d are the same for the buildings classified
 136 into the same structural typology.

137 iii. Determination of vulnerability index limits (V_a and V_b)

138 According to Aguilar-Mélendez et al. (2019a), V_a and V_b , define the minimum and maximum values,
 139 respectively, that can take V (see Eq. 3 and the explanation of Eq.3 in step iv. A detailed description
 140 is also available in Aguilar-Mélendez et al. 2019a). For instance, in previous studies, Aguilar-
 141 Mélendez et al. (2019a,b) adopted -0.04 for V_a and 1.04 for V_b , for studying the Barcelona case. The
 142 election of these previous values was also based on previous works (Lantada 2007; Aguilar-
 143 Mélendez et al. 2019b). We also used these same values for V_a and V_b in the present study for the
 144 reasons mentioned above.

145 iv. Calculation of Beta *pdf* parameters: α_m and β_m

146 The parameters previously determined are used to compute α_m and β_m . These last values complete
 147 the required information to define the Beta *pdf* function representing the seismic vulnerability of
 148 each analyzed building.

149 In this step, values of β_m between 0.1 and 8 are assumed. This specific range was selected by Aguilar-
 150 Meléndez et al. (2019a.) as a result of a sensitivity analysis. The primary purpose of selecting this
 151 range was to reduce the calculation time because, according to the sensitivity analysis, values
 152 between 0.1 and 8 were enough to consider a wide variety of beta functions used to represent the
 153 seismic vulnerability of buildings. However, any user of the methodology could consider a different
 154 range of values of β_m . The increment between values of β_m depends on the desired resolution. Then,
 155 for each β_m , the corresponding α_m pair is computed using Eq. (2). In this process, we calculated the
 156 integral in Eq. (3) for each (α_m, β_m) pair. The final (α_m, β_m) pair correspond to the pair closest to the
 157 0.9 value.

$$\alpha_m = \left(-\beta_m \cdot \frac{\bar{V}_l - V_a}{V_b - V_a} \right) / \left(\left(\frac{\bar{V}_l - V_a}{V_b - V_a} - 1 \right) \right) \quad (2)$$

158

$$0.9 = \int_{y_1}^{y_2} f(y) dy = B_{y_2}(\alpha_m, \beta_m) - B_{y_1}(\alpha_m, \beta_m) \quad (3)$$

159 where $y_1 = V_c$; $y_2 = V_d$; $B_{y_2}(\alpha_m, \beta_m)$ is the incomplete Beta function (beta cumulative distribution
 160 function (CDF)) for y_2 ; $B_{y_1}(\alpha_m, \beta_m)$ is the CDF for y_1 . Finally, in this step, the computed beta function's
 161 mean and standard deviation are determined according to Equations (4) and (5), respectively. A
 162 similar procedure described by Aguilar-Mélendez et al. (2019a) is performed to determine the other
 163 two seismic vulnerability functions: the lower and the upper.

$$Mean = (V_b - V_a) \left(\frac{\alpha_m}{\alpha_m + \beta_m} \right) + V_a \quad (4)$$

164

$$\sigma_{\bar{V}} = \sqrt{\frac{\alpha_m \beta_m}{(\alpha_m + \beta_m)^2 (\alpha_m + \beta_m + 1)} \cdot (V_b - V_a)^2} \quad (5)$$

165

2.1.3. Seismic risk in the VIM_P

166 According to the VIM_P, the seismic risk is computed with Eq. (6), and the results are annual
 167 frequencies of exceedance (ν) for each non-null damage grade (D_k). There are five non-null damage
 168 grades. The damage grade 5 means the total collapse of the building.

$$\nu[D > D_k] \approx \sum_I \sum_V P[D > D_k | V, I] P[V] \gamma'[I] \quad (6)$$

169 where $P[D > D_k | V, I]$ = probability that damage (D) is greater than D_k for a building with a
 170 vulnerability index (V), that receives the effects of an earthquake with a macroseismic intensity (I)
 171 (Aguilar-Mélendez et al. 2019a). This probability of damage is assessed by applying the damage
 172 function defined in previous works (Lagomarsino and Giovinazzi 2006; Milutinovic and Trendafiloski
 173 2003; Giovinazzi 2005).

174 $P[V]$ = probability of V . Value computed from the seismic vulnerability functions from each studied
 175 building;

176 $\gamma'[I]$ = annual frequency of exceedance of I (Aguilar-Mélendez et al. 2019a). Value determined
 177 from the seismic hazard curve.

178 In the following sections, we include the description of the essential data used to apply the VIM_P.
 179 We also highlight relevant results of seismic vulnerability of Ciutat Vella and Nou Barris's districts.
 180 Additionally, we include the main values of the seismic risk results for the same districts of
 181 Barcelona.

182

2.1.4. The VIM_P versus the Capacity Spectrum-Based method to assess seismic risk

The VIM_P methodology has shown to be robust to assess seismic risk, and its application has been considered helpful in sites like Barcelona, where a great number of buildings should be evaluated and where seismicity data other than macroseismic intensities are scarce and not enough to cover long return periods. For instance, in this region, there are references of historic earthquakes potentially damaging with significant return periods (Ojeda et al., 2002), and at the same time, there are no acceleration records of seismic ground motions in Barcelona of significant earthquakes. Therefore, the more representative catalog of earthquakes for the region of Barcelona is based on macroseismic intensities data. In the VIM_P, the data in terms of macroseismic intensities can be used directly to compute the seismic hazard using CRISIS2015 (Ordaz et al., 2015) or R-CRISIS (Ordaz et al., 2020). Additionally, the VIM_P applies damage function based on macroseismic intensities and a vulnerability index; therefore, the data of the earthquakes and the damage functions are consistent (macroseismic intensities) and robust.

The VIM_P methodology is a derivation of the VIM that allows determining seismic risk scenarios. The VIM methodology is related to valuable and extensive work developed in the last 25 years in different countries with emphasis on some European countries as Italy, Spain, Greece, among many others (see for instance Vacareanu et al., 2004; Faccioli et al., 2004; Giovinazzi, 2005; Lagomarsino and Giovinazzi, 2006; Barbat et al., 2006; Dolce et al., 2006; Bernardini, 2007a, b; Barbat et al., 2009; Vicente et al., 2011; Neves et al., 2012; Ferreira et al., 2013, 2017a,b; Athmani et al. 2015; Guardiola-Víllora and Basset-Salom 2015, 2020; Ruiz et al. 2015; Cherif et al. 2016; Lestuzzi et al. 2016; Maio et al., 2016; Apostol et al., 2019; Giuliani et al., 2019; Ortega et al., 2019; Ademović et al. 2020; Basset-Salom and Guardiola-Víllora, 2020; Kassem et al., 2020; Romis et al., 2020; Taibi et al., 2020). Recently, Aguilar-Meléndez et al. (2019a) highlighted that the seismic risk results obtained according to the VIM_P agree with the results determined through the application of the VIM. Similarly, Lantada et al. (2009) developed a comparison between the VIM method and the capacity spectrum-based method (CSBM). They determined a good correlation between the seismic results determined by the VIM and CSBM methods. However, because of the difficulty of getting detailed structural information about a great number of buildings, the VIM method showed a better resolution and detail of the damage scenarios. For these reasons, it is possible to affirm that VIM and VIM_P allow determining reasonable values of the seismic risk of buildings in urban areas. Moreover, the results obtained are compatible with, but more resolute than, those obtained applying the CSBM methods. According to this, it is possible to affirm that the VIM_P is a robust methodology that allows obtaining good results about the seismic risk of buildings. In the next section, we describe the application of the VIM_P to assess the seismic risk of the residential buildings of two districts of the city of Barcelona.

2.2. Seismic hazard in Barcelona

We performed a PSHA for Barcelona considering the seismic sources (Figure 2) and seismicity data (Table 3) utilized by Aguilar-Melendez et al. (2019a); however, in this case, we apply new GMPEs (Ground Motion Prediction Equations). This section describes the primary data used to compute the seismic hazard and the main results obtained.

224 *Seismic sources*

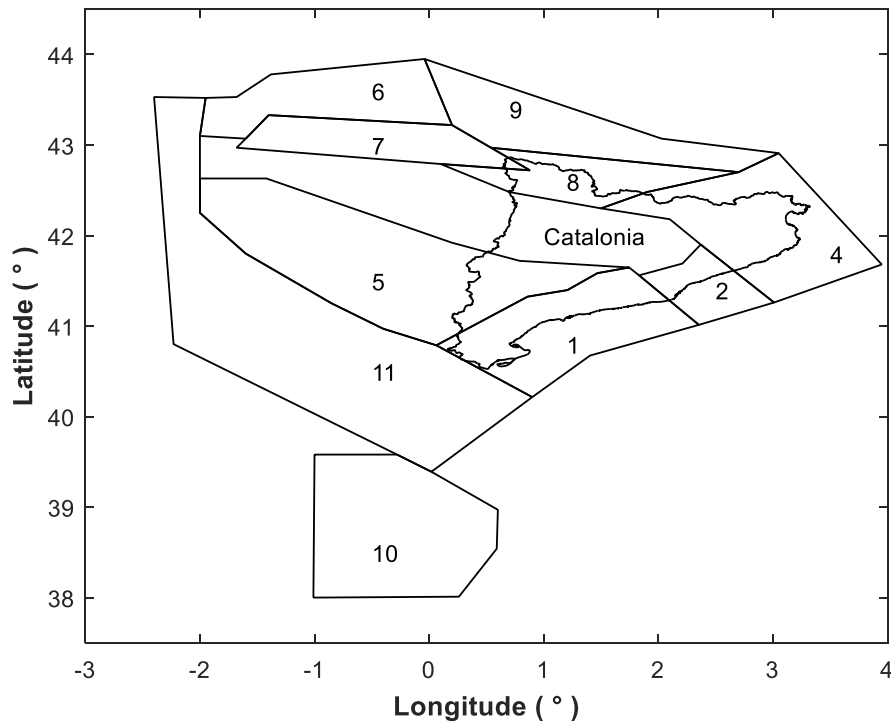
225 The geometry of the seismic sources used in the present study is shown in Figure 2. Moreover, the
 226 seismicity of these sources was represented according to the truncated Gutenberg-Richter relation
 227 (see Eq. (7)). For this last purpose, the seismic parameters of the seismic sources of Figure 2 (Table
 228 3) were determined according to an earthquake catalog based on macroseismic intensities (Secanell
 229 et al., 2004). The seismic sources and their respective seismicity parameters have been used in
 230 different studies of the seismic hazard of Barcelona and Catalonia (Irizarry et al., 2011; Secanell et
 231 al., 2004; Irizarry, 2004).

232 On the other hand, R-CRISIS allows computing directly seismic hazard in terms of macroseismic
 233 intensities. Therefore, and mainly because these are the only representative seismicity data for the
 234 studied areas, we choose this option to compute the seismic hazard of Barcelona. In other words,
 235 we assigned directly to R-CRISIS the geometry of the seismic sources of Figure 2 and its respective
 236 seismicity parameters in terms of macroseismic intensities (Table 3).

237

$$\lambda(I) = \alpha \frac{e^{-\beta(I-I_{min})} - e^{-\beta(I_{max}-I_{min})}}{1 - e^{-\beta(I_{max}-I_{min})}} \quad (7)$$

238 where $\lambda(I)$ is the annual frequency of exceedance of the macroseismic intensity I , I_{min} is the
 239 minimum epicentral intensity considered, I_{max} is the maximum epicentral intensity for each zone,
 240 α is the annual frequency of exceedance of intensities greater or equal to I_{min} , and β is the slope
 241 related to the Gutenberg-Richter law (Goula et al., 1997; Ordaz et al., 2020).



242
 243

Figure 2. Seismic sources considered to compute the seismic hazard of Barcelona.

244 *Ground Motion Prediction Equation*

245 Mezcuca et al. (2020) recently developed new GMPEs for Spain. These GMPEs were developed
 246 considering more than 3700 intensities data. The GMPEs developed allows computing values of
 247 macroseismic intensities for Spain. In this work, we applied two of the four GMPEs determined by
 248 Mezcuca et al. (2020), the Pyrenees and the SCR (Stable Continental Region), because these two
 249 GMPEs (Mezcuca et al., 2020) are enough to cover the regions of the seismic sources that were
 250 considered in the present work.

251

252 *Table 3. Seismicity parameters of the seismic sources of Figure 2. Adapted from Secanell et al. (2004)*

Seismic source	α	$\sigma(\alpha)^*$	β	$\sigma(\beta)^*$	h (km)*	I_{min}^*	I_{max}^*	I_{max} observed *
1	0.100	0.030	1.864	0.559	7	V	VIII	VII
2	0.128	0.033	1.608	0.324	7	V	IX	VIII
4	0.157	0.030	1.256	0.186	10	V	X	IX
5	0.040	0.014	1.319	0.373	10	V	IX	VIII
6	0.099	0.025	1.977	0.640	10	V	VII	VI
7	0.957	0.090	1.420	0.116	15	V	X	VIII
8	0.218	0.040	1.716	0.246	15	V	IX	VIII
9	0.070	0.020	1.737	0.214	10	V	VIII	VII
10	0.635	0.059	1.201	0.083	10	V	XI	X
11	0.060	0.016	0.886	0.242	10	V	IX	VIII

253 * $\sigma(\alpha)$ is the estándar deviation of α ; $\sigma(\beta)$ is the standard deviation of β ; h is the depth in km; I_{min} is the
 254 minimum epicentral intensity assigned to the seismic source; I_{max} is the maximum epicentral intensity assigned
 255 to the seismic source; I_{max} observed is the maximum epicentral intensity observed in the seismic source.

256

257 *Table 4. Ground Motion Predictions Equations determined by Mezcuca et al. (2020)*

Zone	Average intensity	Standard Deviation
Stable Continental Region	$-0.223 + 1.347M - 0.0023R - 1.235\log R$	0.59
Pyrenees	$-2.559 + 1.774M - 0.0062R - 0.933\log R$	0.60

258

259 *Local site effects*

260 Figure 3 shows the surface geological features of different areas of the city of Barcelona. These
 261 geological features were considered by Cid et al. (1999) to define the five seismic zones shown in
 262 Figure 4: Rock, Soil type I, Soil type II, Soil type III, and artificial soil (A). Rock seismic zone
 263 corresponds to rocky outcrops. Zone I corresponds to Holocene outcrops. Meanwhile, zone II
 264 corresponds to Pleistocene outcrops with a tertiary substrate. Otherwise, zone III corresponds to
 265 Pleistocene outcrops without tertiary substrate. Finally, seismic zone A corresponds to artificial soil.
 266 With these references and considering the work of Lantada 2007 and Aguilar-Meléndez et al.
 267 2019a,b, we also considered for the present work the criteria of increasing in a half degree the
 268 macroseismic intensities in rock to determine the macroseismic intensities in soil sites.

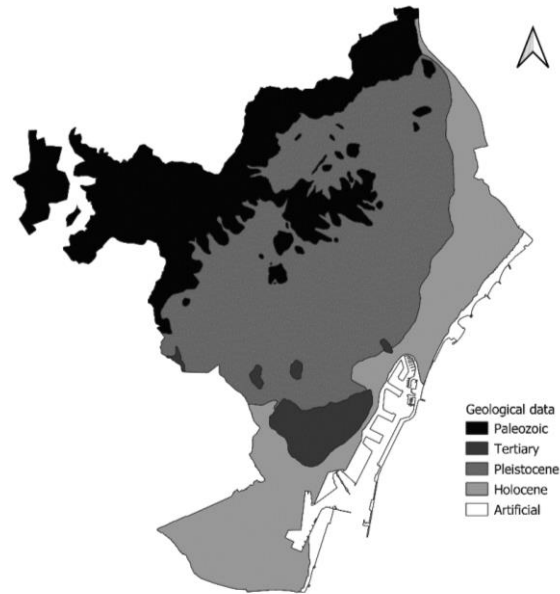


Figure 3. Surface geological features in the city of Barcelona, according to Cid et al. (1999)

269
270

271

272 *Seismic hazard results*

273 Figure 5 includes seismic hazard curves for the city of Barcelona for two cases, curves computed by
 274 Aguilar-Melendez et al. 2019a and curves computed in the present work. As was mentioned
 275 previously, the main difference in both cases is the GMPEs used. In the first case, GMPEs of López-
 276 Casado et al. (2000) were applied, and in the second case (present work), GMPEs of Mezcua et al.
 277 (2020) were used.

278

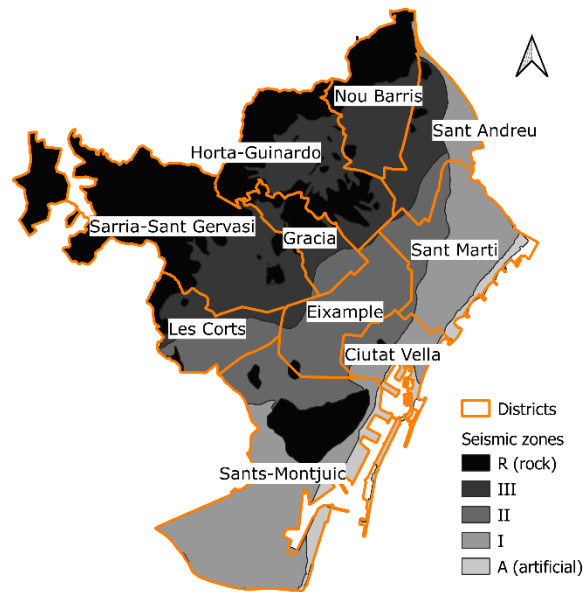
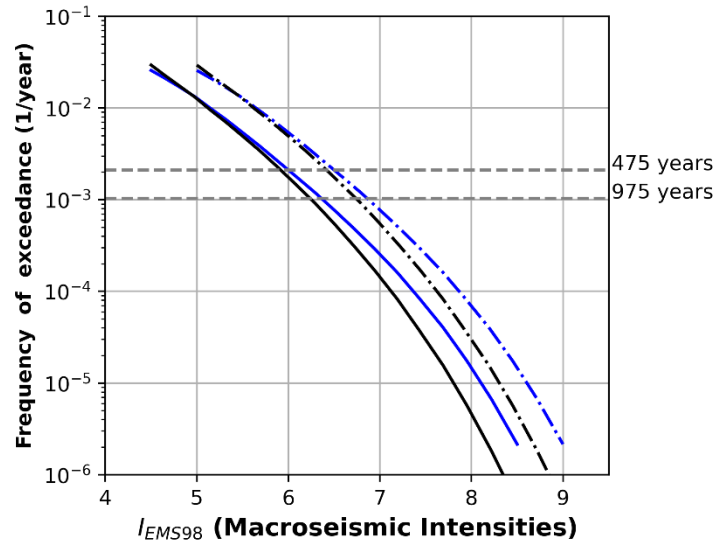


Figure 4. Districts of the city of Barcelona and seismic zones (Cid et al., 1999)

279
280



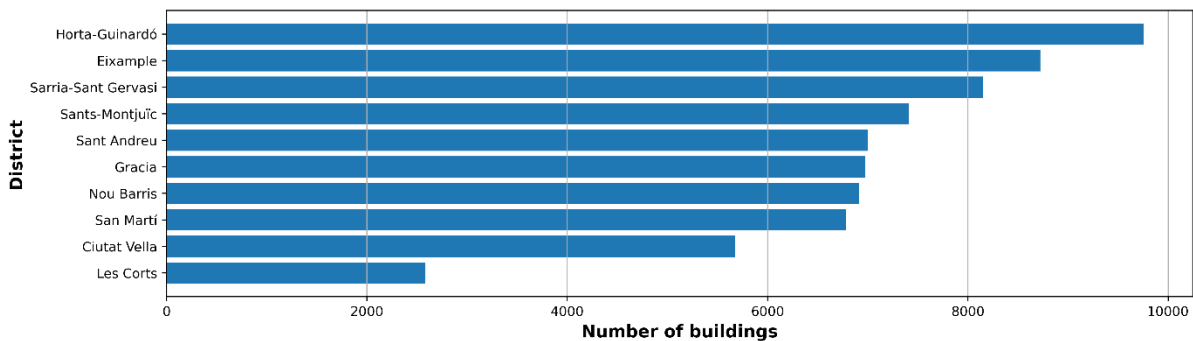
281

282 *Figure 5. Curves of seismic hazard for Barcelona’s rock sites (continuous black line this work and continuous blue line*
 283 *Aguilar-Meléndez et al. 2019a), and Seismic hazard curves for Barcelona’s soil sites (dotted black line this work and dotted*
 284 *blue line Aguilar-Meléndez et al. 2019a).*

285 **2.3. Data of the residential buildings of Barcelona**

286

287 We used the same building database of Barcelona that was used by Aguilar-Meléndez et al. (2019a).
 288 According to this data, the number of residential buildings in Barcelona’s districts ranges
 289 approximately from 2500 to 10000 (see Figure 6). The district of Ciutat Vella has 5675 residential
 290 buildings, and in the Nou Barris district, there are 6916 residential buildings.



291

292 *Figure 6. Number of buildings of each district of Barcelona*

293 The database of Barcelona’s buildings (Aguilar-Meléndez et al. 2019a,b; Lantada et al. 2010, 2018)
 294 that we used to assess seismic vulnerability and seismic risk includes the information listed in Table
 295 5. It is essential to highlight that this database has typologies valid for both the VIM method
 296 (Milutinovic and Trendafiloski, 2003) and the VIM_P method (Aguilar-Meléndez et al. 2019a).

297 The more common structural materials of the residential buildings in Barcelona are masonry and
 298 reinforced concrete, with 69.8% and 26.2%, respectively (Figure 7). Similarly, we analyzed Ciutat

299 Vella and Nou Barris’s residential buildings’ data, and we observed that the proportion of buildings
 300 according to their primary structural material is similar between Barcelona (Figure 7) and its Nou
 301 Barris district (Figure 7). Additionally, we identified that the Ciutat Vella district has a significantly
 302 higher proportion of masonry buildings (88.5%) than the percentage of masonry buildings in
 303 Barcelona’s whole city (69.8%).

304 *Table 5. Basic information of the database of the residential buildings in Barcelona*

Datum	
1	Id of the building
2	Cadastral plot code
3	Sub-District code
4	District code
5	Stories of the building
6	Structural Typology
7	Construction year
8	Seismic Zone
9	Conservation state
10	Building position in the block

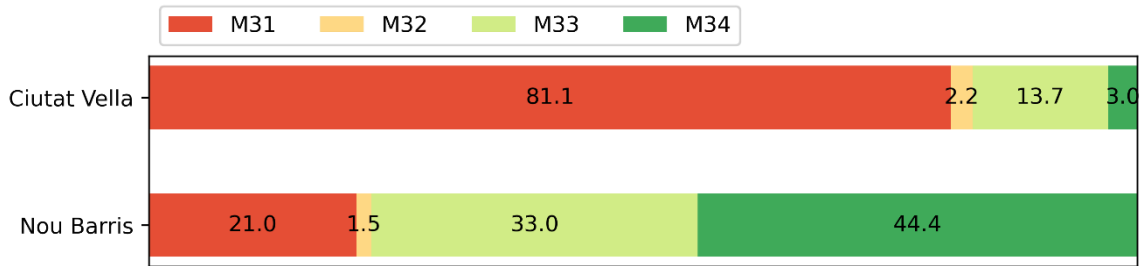
305
 306 If we analyze the typologies distribution by district, we can observe significant differences in the
 307 distribution of the masonry typologies of the buildings in Ciutat Vella and Nou Barris. For instance,
 308 in Ciutat Vella, the M31 typology is the most common typology, with 81.1% of the masonry buildings
 309 (Figure 8). However, this typology represents only 21.0% of the masonry buildings in Nou Barris
 310 (Figure 8). In this last district, the most common typology is the M34 typology, with 44.4% of the
 311 masonry buildings (Figure 8).



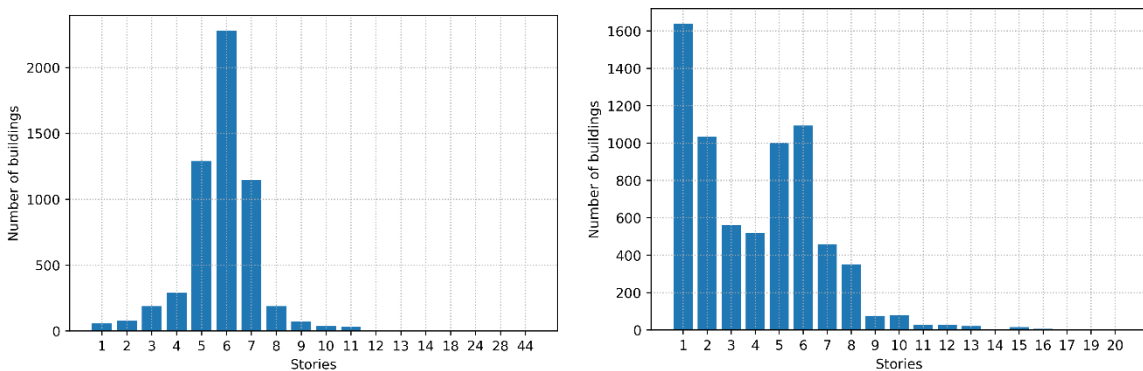
312
 313 *Figure 7. Distribution (%) of buildings by primary structural material (M-Masonry, S-Steel, RC-Reinforced Concrete, W-*
 314 *Wood) for 69982 buildings in Barcelona, 5675 buildings in Ciutat Vella, and 6916 buildings in Nou Barris.*

315 Other relevant information in the database is the year of construction of each building. Based on
 316 this last information, we determined that Ciutat Vella and Nou Barris’s buildings have a mean age
 317 of 119.58 years and 59.88 years, respectively. Similarly, the mean number of stories of residential
 318 buildings equals 5.85 stories in Ciutat Vella and 4.03 in Nou Barris. The detailed distribution of the
 319 buildings by the number of stories in Ciutat Vella and Nou Barris is shown in Figure 9. Moreover, it
 320 is possible to observe in Figure 9 differences between the buildings’ distributions according to their
 321 stories in Ciutat Vella and Nou Barris. For instance, the most common buildings in Ciutat Vella have
 322 six stories (40.22%), while in Nou Barris, the most frequent buildings have one story (23.68%).

323 Additionally, it is possible to note in Ciutat Vella that buildings with 5, 6, and 7 stories represent
 324 83.15% of this district's residential buildings.



325
 326 *Figure 8. Distribution (%) of masonry buildings by structural typology (according to the Risk-UE building typology matrix)*
 327 *in Ciutat Vella and Nou Barris.*



328
 329 *Figure 9. Distribution of buildings by their stories in Ciutat Vella (left) and Nou Barris (right).*

330 2.4. Seismic vulnerability of Ciutat Vella and Nou Barris

331
 332 It is essential to highlight that, as was mentioned previously (section 2.1.2), a part of the procedure
 333 to compute seismic vulnerability functions includes the assessment of the mean vulnerability index
 334 (Eq. (1)). This mean value depends on three elements: a) the structural typology, b) building regional
 335 modifiers, and c) building-specific modifiers.

336
 337 Eq. (1) was assessed to determine the seismic vulnerability of each building that was studied in the
 338 present work. For this last purpose, we considered the following conditions: a) the first term of Eq.
 339 (1) depends on the structural typology of each building according to the typologies of Table 6
 340 (Milutinovic and Trendafiloski, 2003); b) to assess the second term of Eq. (1), the regional modifiers
 341 that were defined by Lantada (2007) for the buildings of Barcelona were applied (Table 7), and, c)
 342 the building-specific modifiers were considered according to the modifiers proposed by Lantada
 343 (2007).

344
 345 In the following part of this section, we included an example of the data and the procedure applied
 346 to compute seismic vulnerability of the buildings of the districts of Ciutat Vella and Nou Barris. For
 347 this purpose, we selected four buildings from the complete database of the residential buildings of
 348 Ciutat Vella and Nou Barris districts in Barcelona city (Table 8). Subsequently, we applied the VIM_P
 349 and used the data in Table 8 to compute the seismic vulnerability functions representing the four

350 buildings' seismic vulnerability. Table 9 shows the parameters that define the vulnerability functions
 351 computed, and in Figure 10, it is possible to observe the respective seismic vulnerability curves.
 352

353 The vulnerability curves of Figure 10 are an input to compute the seismic risk of the buildings of
 354 Table 8. However, the vulnerability curves by themselves describe the seismic vulnerability of the
 355 buildings. For instance, the probability that in the CV1 building, the vulnerability index will be greater
 356 than 0.8 is equal to 50%, 65%, and 79%, according to the lower, best, and upper seismic
 357 vulnerability, respectively. Similarly, the probability that in the CV2 building, the vulnerability index
 358 will be greater than 0.8 is equal to 27%, 46%, and 63% according to the lower, best, and upper
 359 seismic vulnerability, respectively. Therefore, it is possible to conclude that building CV1 is
 360 seismically more vulnerable than building CV2. Similarly, the probability that in the NB1 and NB2
 361 buildings, the vulnerability will be greater than 0.8 is equal to 40% and 21%, respectively, if only the
 362 best vulnerability curve is considered.

363
 364

Table 6. Structural Typologies (Milutinovic and Trendafiloski, 2003).

Group	Typology	Description	Representative values of vulnerability**				
			V_I^{min}	V_I^-	V_I^*	V_I^+	V_I^{max}
Mason ry	M31	Unreinforced masonry bearing walls with wooden slabs	0.460	0.650	0.740	0.830	1.020
	M32	Unreinforced masonry bearing walls with masonry vaults	0.460	0.650	0.776	0.953	1.020
	M33	Unreinforced masonry bearing walls with composite steel and masonry slabs	0.460	0.527	0.704	0.830	1.020
	M34	Unreinforced masonry bearing walls with reinforced concrete slabs	0.300	0.490	0.616	0.793	0.860
Concre te	RC32	Irregular concrete frames with unreinforced masonry infill walls	0.060	0.127	0.522	0.880	1.020
Steel	S3	Steel frames with unreinforced masonry infill walls	0.140	0.330	0.484	0.640	0.860
	S5	Steel and RC composite systems	-0.020	0.257	0.402	0.720	1.020
Wood	W	Wood	0.140	0.207	0.447	0.640	0.860

365 ** V_I^* is the more probable value of the vulnerability index for the corresponding typology. V_I^- and V_I^+ delimit the range
 366 of the probable values of the vulnerability index for the corresponding typology. V_I^{min} and V_I^{max} increase the range of the
 367 probable values of the vulnerability index in order to include the less probable values of the vulnerability index for the
 368 same typology.

369
 370
 371

Table 7. Regional modifiers for buildings in Barcelona (Lantada, 2007)

Period	M31	M32	M33	M34	RC32
<=1940	+0.198	+0.162	+0.234	-	-
1941-1962	+0.135	+0.099	+0.171	-	-
1963-1968	+0.073	+0.037	+0.109	+0.134	+0.228
1969-1974	+0.010	-0.026	+0.046	+0.009	+0.103
1975-1994	-0.052	-0.088	-0.016	-0.053	-0.022
1995-2002	-0.052	-0.088	-0.016	-0.053	-0.022
>2002	-0.052	-0.088	-0.016	-0.053	-0.022

372 Table 8. Example of the primary data of each residential building of Barcelona used to determine their seismic vulnerability.

No.	Data	Building 1 in Ciutat Vella (CV1)	Building 2 in Ciutat Vella (CV2)	Building 1 in Nou Barris (NB1)	Building 2 in Nou Barris (NB2)
1	Structural typology	M31	M33	M31	RC32
2	Reliability parameter	8	8	8	8
3	Conservation state	Normal	Normal	Normal	Normal
4	Stories of the building	6	4	6	7
5	Construction year	1965	1969	1987	2004
6	Seismic Zone (Terrain)	II(Soil)	II(Soil)	III(Soil)	R(Rock)

373

374 According to Aguilar-Meléndez et al. (2019a), the seismic vulnerability of groups of buildings can
 375 also be represented using vulnerability functions. Therefore, for the previous example, it could be
 376 possible, for instance, to obtain vulnerability functions that represent the seismic vulnerability of
 377 the two buildings of Ciutat Vella and the two buildings of Nou Barris. Figure 11 shows the case of
 378 the vulnerability curves that represent the seismic vulnerability of the two buildings of Ciutat Vella.

379

380

Table 9. Parameters that define the vulnerability functions of the residential buildings of Table 8

Building	<i>Lower</i>				<i>Best</i>				<i>Upper</i>			
	α	β	Mean	SD	α	β	Mean	SD	α	β	Mean	SD
CV1	4.21	1.41	0.77	0.18	4.68	1.11	0.83	0.16	5.31	0.81	0.90	0.14
CV2	4.76	2.41	0.68	0.18	4.11	1.51	0.75	0.19	4.41	1.11	0.82	0.17
NB1	4.20	2.31	0.66	0.19	4.46	1.81	0.73	0.18	4.22	1.21	0.80	0.18
NB2	0.68	1.01	0.39	0.32	1.16	1.11	0.51	0.30	1.32	0.81	0.63	0.30

381

382 In the present work, we applied the VIM_P to determine the vulnerability functions of 5675
 383 residential buildings in Ciutat Vella and 6916 in Nou Barris. To do this, first, the three vulnerability
 384 functions (lower, best, and upper) for each studied building were obtained. After that, we used
 385 these individual vulnerability functions to determine average vulnerability functions for different
 386 groups of buildings. The selection of the different groups had the objective of analyzing the influence
 387 of different features in the seismic vulnerability of the studied buildings. The total number of groups
 388 analyzed with their respective features is summarized in Table 10 and Table 11. These two tables
 389 also indicate the data used to analyze each group or subgroup of buildings.

390 To determine the seismic vulnerability of the groups of buildings in Table 10 and Table 11, according
 391 to the VIM_P, the procedure defined by Aguilar-Meléndez (2011) and Aguilar-Meléndez et al.
 392 (2019a) was applied. The procedure can be summarized in two steps: Step 1. Determination of three
 393 vulnerability functions for each building of the group according to the VIM_P and Step 2.
 394 Determination of three representative vulnerability functions for the whole residential buildings in
 395 this group, based on the vulnerability functions computed in Step 1.

396

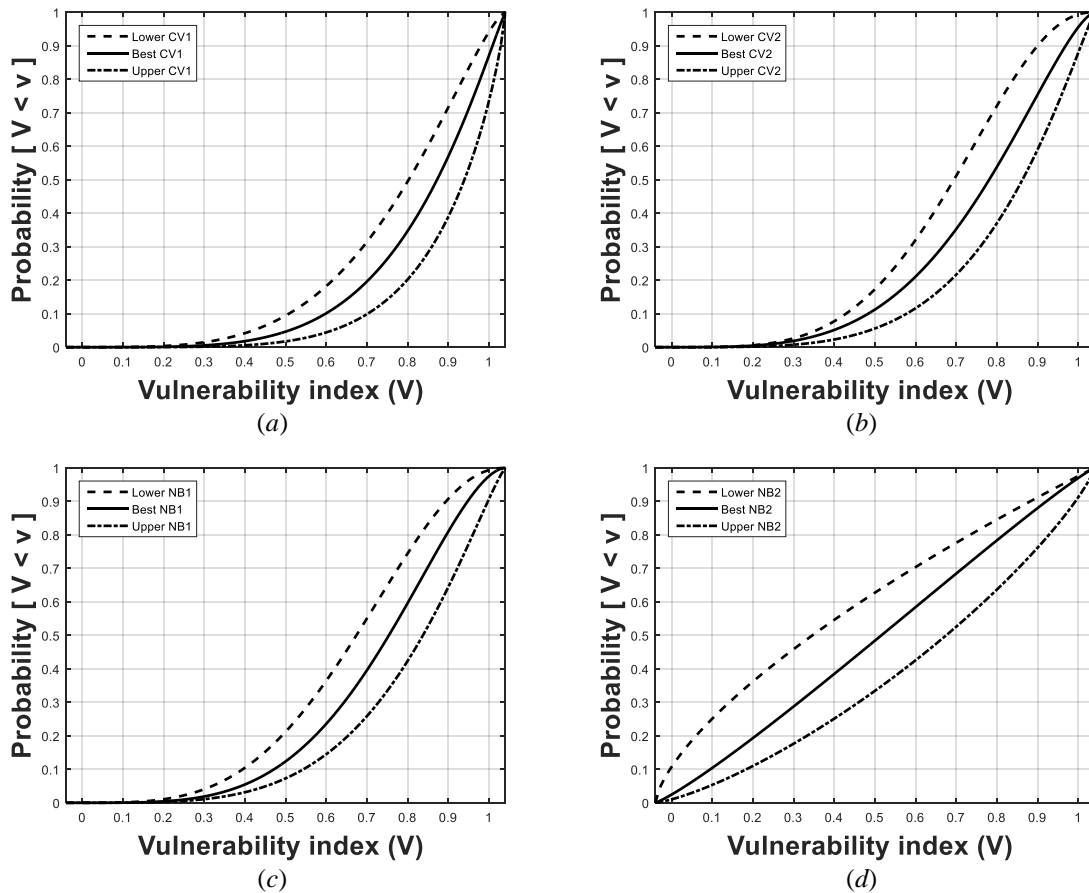


Figure 10. Vulnerability functions of the buildings of Table 8. Building CV1 (a), building CV2 (b), building NB1 (c), and building NB2 (d).

397
398

399 To compute the seismic vulnerability according to the VIM_P, we applied the USERISK2015 software
 400 (Aguilar-Meléndez et al. 2016). Figure 12 shows the seismic vulnerability curves for Ciutat Vella and
 401 Nou Barris districts that were also determined by Aguilar-Meléndez et al. (2019b). However, in this
 402 work, we performed a more extensive assessment of the seismic vulnerability of the buildings of
 403 Ciutat Vella and Nou Barris because, in this work, we assessed new seismic vulnerability curves of
 404 sub-groups of these dwelling buildings (Table 10 and Table 11). Figure 12 includes the seismic
 405 vulnerability curves that describe the seismic vulnerability for 5675 residential buildings in Ciutat
 406 Vella (GCV1) and 6916 residential buildings of Nou Barris (GNB1). Using these results, we can affirm
 407 that the mean vulnerability index for the *Best* curve for Ciutat Vella buildings is 0.90 (Figure 12). We
 408 also can determine that the probability that a building in Ciutat Vella has a vulnerability index
 409 greater than 0.8 would be 73.52%, 83.59%, and 88.37%, counting the *Lower*, *Best*, and *Upper*
 410 vulnerability curves, respectively. Similarly, we can observe that the mean vulnerability index for
 411 the *Best* curve for Nou Barris buildings is 0.69 (Figure 12). Simultaneously, the probability that a
 412 residential building in Nou Barris has a vulnerability index greater than 0.8 would be 21.33%, 34.03%,
 413 and 52.14 %, if the *Lower*, *Best*, and *Upper* vulnerability curves are considered, respectively.

414

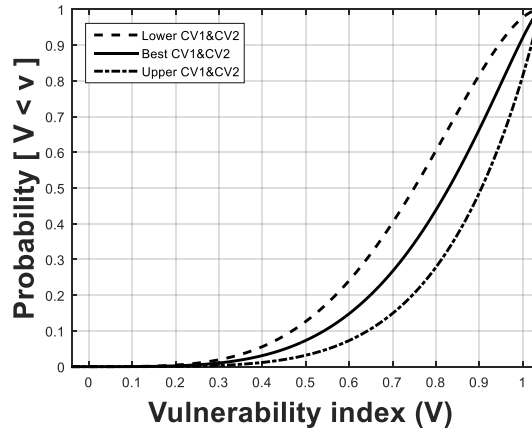


Figure 11. Vulnerability functions of a group of two buildings of Ciutat Vella (CV1 and CV2)

415
416

417

Table 10. Group and subgroups of buildings of the district of Ciutat Vella that were studied in the present work.

ID	Group	Subgroup	Number of residential buildings in the group or subgroup	Steps of the procedure to obtain the vulnerability functions	Data considered to compute the vulnerability functions	Number of vulnerability functions determined
GCV1	Ciutat Vella		5675	Step 1*	***	17025
				Step 2**	****	3 (Figure 12)
GCV2		Ciutat Vella Masonry	5022	Step 1*	***	15066
				Step 2**	****	3 (Figure 14a)
GCV3		Ciutat Vella RC	459	Step 1*	***	1377
				Step 2**	****	3 (Figure 14b)
GCV4		Ciutat Vella M31	4069	Step 1*	***	12207
				Step 2**	****	3 (Figure 15)
GCV5		Ciutat Vella M31<1969	3993	Step 1*	***	11979
				Step 2**	****	3 (Figure 16a)
GCV6		Ciutat Vella M31>=1969	76	Step 1*	***	228
				Step 2**	****	3 (Figure 16b)
GCV7		Ciutat Vella Stories<6	1908	Step 1*	***	5724
				Step 2**	****	3 (Figure 13a)
GCV8		Ciutat Vella Stories >=6	3767	Step 1*	***	11301
				Step 2**	****	3 (Figure 13b)

418

* Assessment of three vulnerability functions for each building according to the VIM_P

419

** Assessment of three representative vulnerability functions for the whole residential buildings in this group, based on the vulnerability functions determined in step 1.

420

*** The six data of each building as the data mentioned in Table 8.

421

**** The vulnerability functions of each building that were obtained in step 1.

422

423

It is essential to highlight that the VIM_P computes the seismic vulnerability of each building considering the structural typology and the additional data mentioned in Table 8. And the seismic vulnerability results are vulnerability functions in terms of probability of non-exceedance of the vulnerability index. Therefore, because all the vulnerability functions are in the same units, it is possible to use these vulnerability functions to compute representative seismic vulnerability curves of groups of buildings with different structural typologies (see also Aguilar-Meléndez et al. 2019a).

424

425

426

427

428

429

430

Table 11. Group and subgroups of buildings of the district of Nou Barris that were studied in the present work.

ID	Group	Subgroup	Number of residential buildings in the group or subgroup	Steps of the procedure to obtain the vulnerability functions	Data considered to compute the vulnerability functions	Number of vulnerability functions determined
GNB1	Nou Barris		6916	Step 1*	***	20748
				Step 2**	****	3 (Figure 12).
GNB2		Nou Barris Masonry	4885	Step 1*	***	14655
				Step 2**	****	3 (Figure 14c)
GNB3		Nou Barris RC	1761	Step 1*	***	5283
				Step 2**	****	3 (Figure 14d)
GNB4		Nou Barris M31	1026	Step 1*	***	3078
				Step 2**	****	3 (Figure 15)
GNB5		Nou Barris M31<1969	961	Step 1*	***	2883
				Step 2**	****	3 (Figure 16c)
GNB6		Nou Barris M31>=1969	65	Step 1*	***	195
				Step 2**	****	3 (Figure 16d)
GNB7		Nou Barris Stories<6	4757	Step 1*	***	14271
				Step 2**	****	3 (Figure 13c)
GNB8		Nou Barris Stories >=6	2159	Step 1*	***	6477
				Step 2**	****	3 (Figure 13d)

431

* Assessment of three vulnerability functions for each building according to the VIM_P

432

** Assessment of three representative vulnerability functions for the whole residential buildings in this group, based on the vulnerability functions determined in step 1.

433

*** The six data of each building as the data mentioned in Table 8.

434

**** The vulnerability functions of each building that were obtained in step 1.

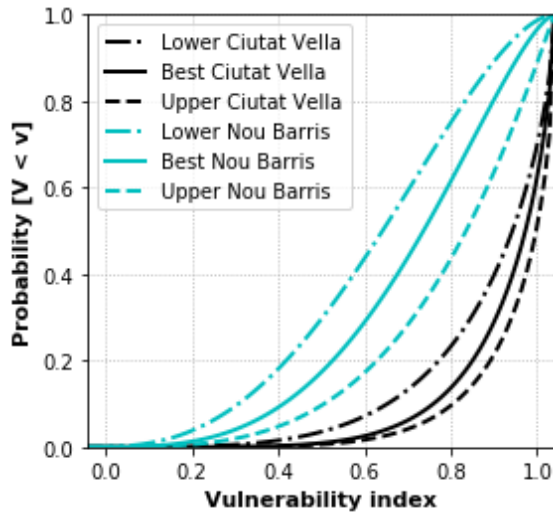
435

436

437

In this study, we computed the seismic vulnerability curves of two groups of buildings that were defined, taking into account the number of stories of the buildings (Figure 13): a) buildings with five or fewer stories, and b) buildings with six or more stories. Figure 13 and Table 12 summarize the results for the groups of buildings defined according to their number of stories. These results indicate that the mean vulnerability index of the *Best* curve of seismic vulnerability is equal to 0.87 and 0.91 for Ciutat Vella buildings with less than six stories (GCV7) and more than five stories (GCV8), respectively. Similarly, in Nou Barris, we obtained that the mean vulnerability index of the *Best* curve of seismic vulnerability is equal to 0.7 and 0.67 for buildings with less than six stories (GNB7) and more than five stories (GNB8), respectively.

446



Seismic Vulnerability Curves for the group of buildings*		α	β	Mean	SD
Ciutat Vella (GCV1)	L	3.85	0.63	0.86	0.16
	B	5.62	0.64	0.90	0.12
	U	5.65	0.49	0.92	0.11
Nou Barris (GNB1)	L	2.81	1.77	0.61	0.22
	B	3.40	1.52	0.69	0.21
	U	3.47	1.04	0.77	0.19

*L=Lower, B=Best, U=Upper

447 Figure 12. Seismic vulnerability curves for Ciutat Vella (GCV1) (black lines) and Nou Barris (GNB1) (cyan lines) considering
 448 $V_a=-0.04$ and $V_b=1.04$ (some of the values of the table were published in Aguilar-Meléndez et al. 2019a).
 449

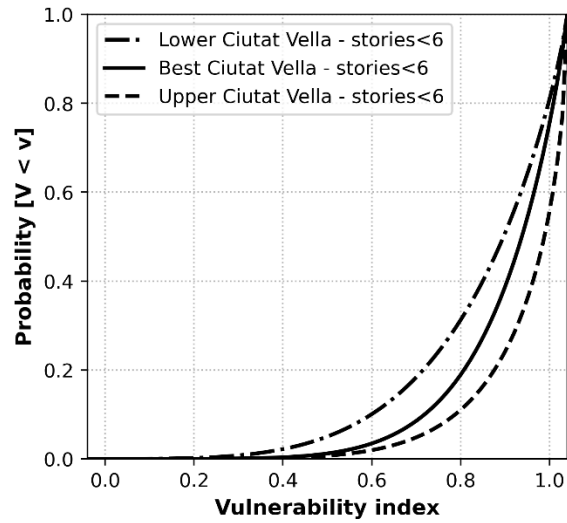
450 Based on the seismic vulnerability results included in Table 12, we observed that in Ciutat Vella, the
 451 buildings with six or more stories (GCV8) are, on average, more vulnerable than the buildings with
 452 fewer than six stories (GCV7). For instance, in Ciutat Vella, the probability that V is greater than 0.8
 453 is equal to 77.40 % and 85.94% (Best curve-Table 12) for buildings with fewer than six stories (GCV7)
 454 and more than five stories (GCV8), respectively. On the other hand, if we consider the Best curve
 455 for the Nou Barris buildings (Table 12), then the probability that V is greater than 0.8 is equal to
 456 34.39% and 33.61% for buildings with fewer than six stories (GNB7) and more than five stories
 457 (GNB8), respectively.

458
 459 Table 12. Probabilities that V exceeds the values of 0.7, 0.8, and 0.9 (probabilities computed from the vulnerability curves
 460 of Figure 13 corresponding to the buidlings of groups).

District	Group of buildings	P(V>0.7) [%]			P(V>0.8) [%]			P(V>0.9) [%]		
		Lower	Best	Upper	Lower	Best	Upper	Lower	Best	Upper
Ciutat Vella	Stories<6 (GCV7)	79.95	90.24	94.47	64.76	77.40	86.69	41.01	51.89	68.91
	Stories>=6 (GCV8)	87.61	93.95	95.58	77.12	85.94	89.13	58.19	68.17	73.74
Nou Barris	Stories<6 (GNB7)	40.13	55.28	70.99	22.04	34.39	52.48	6.99	13.15	27.79
	Stories>=6 (GNB8)	34.72	50.41	67.02	20.10	33.61	51.75	7.41	15.66	31.37

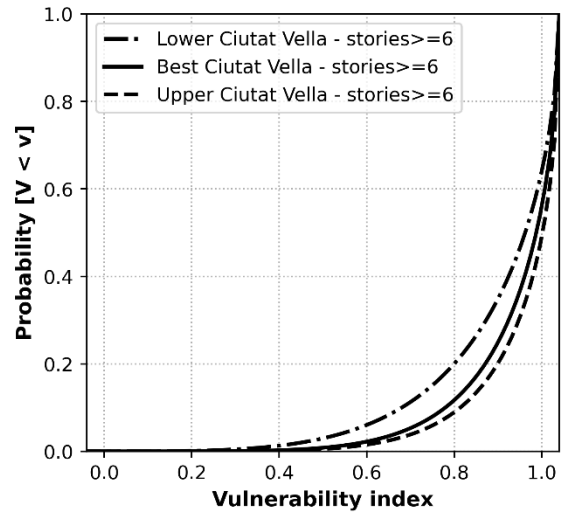
461
 462
 463 Additionally, we determined the seismic vulnerability of masonry and concrete buildings. Figure 14
 464 shows that in Ciutat Vella, there are considerable differences among the vulnerability of masonry
 465 (Figure 14a) and reinforced concrete (RC) buildings (Figure 14b). For instance, if we consider the
 466 best curve, the probability that V is greater than 0.8 is equal to 89.17% and 22.35% for masonry
 467 buildings (GCV2) and RC buildings (GCV3), respectively. This significant difference between the
 468 masonry and RC buildings of Ciutat Vella agrees with the seismic vulnerability results assessed by
 469 Lantada et al. (2018). Remarkably, they applied the VIM for Ciutat Vella’s buildings and obtained a

470 vulnerability index average of 0.59 and 0.93 for reinforced concrete and masonry buildings,
 471 respectively.



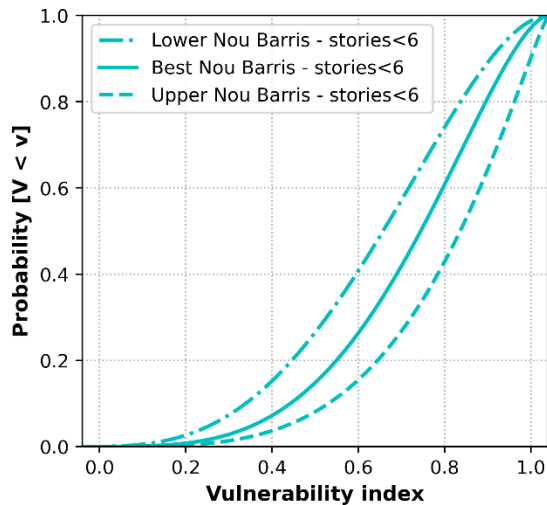
Seismic vulnerability curve	α	β	Mean	SD
Lower	3.98	0.86	0.82	0.17
Best	6.11	0.91	0.87	0.13
Upper	5.66	0.54	0.91	0.11

(a)



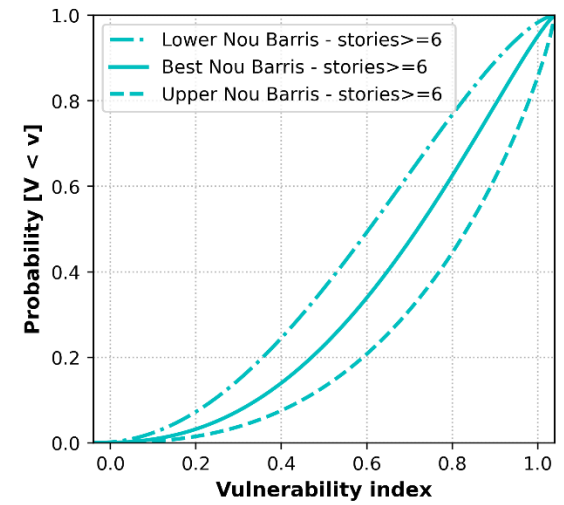
Seismic vulnerability curve	α	β	Mean	SD
Lower	3.78	0.54	0.87	0.16
Best	5.39	0.53	0.91	0.12
Upper	5.64	0.46	0.92	0.11

(b)



Seismic vulnerability curve	α	β	Mean	SD
Lower	3.17	1.88	0.63	0.21
Best	3.91	1.67	0.70	0.19
Upper	3.95	1.15	0.77	0.18

(c)



Seismic vulnerability curve	α	β	Mean	SD
Lower	2.16	1.55	0.58	0.25
Best	2.50	1.23	0.67	0.23
Upper	2.60	0.83	0.76	0.22

(d)

472 Figure 13. Seismic vulnerability curves of buildings in Ciutat Vella with fewer than six stories (GCV7) (a) and with six or more
 473 stories (GCV8) (b) and seismic vulnerability curves of buildings in Nou Barris with fewer than six stories (GNB7) (a) and with
 474 six or more stories (GNB8). For these cases, it was considered $V_a = -0.04$ and $V_b = 1.04$.

475 The vulnerability curves of Figure 14 also show that the masonry buildings of Ciutat Vella (GCV2)
476 (Figure 14a) have, on average, higher levels of seismic vulnerability than the masonry buildings of
477 Nou Barris (GNB2) (Figure 14c). For instance, the *Best* curve indicates that the probability that V
478 is greater than 0.9 is equal to 71.39% and 14.20% for masonry buildings in Ciutat Vella (GCV2) and Nou
479 Barris (GNB2), respectively. The difference between the levels of seismic vulnerability of the average
480 masonry buildings in Ciutat Vella and Nou Barris is because, in the VIM_P, the seismic vulnerability
481 assessment depends on the structural typology and the additional features of the buildings.
482 Therefore, the differences in the percentage of masonry buildings of each structural typology in the
483 districts of Ciutat Vella and Nou Barris are relevant factors that contribute to explain the differences
484 in the average vulnerability of the masonry buildings of both districts. For instance, if only it is
485 considered the structural typology, it is possible to identify (Figure 8) that in Ciutat Vella, the greater
486 percentage of masonry buildings are M31 (81.1%), and in Nou Barris, a similar percentage (77.40%)
487 correspond to the typologies M33 and M34, and these last two typologies have a best vulnerability
488 function that has a V_I^* lower than the M31 structural typology (Table 6).

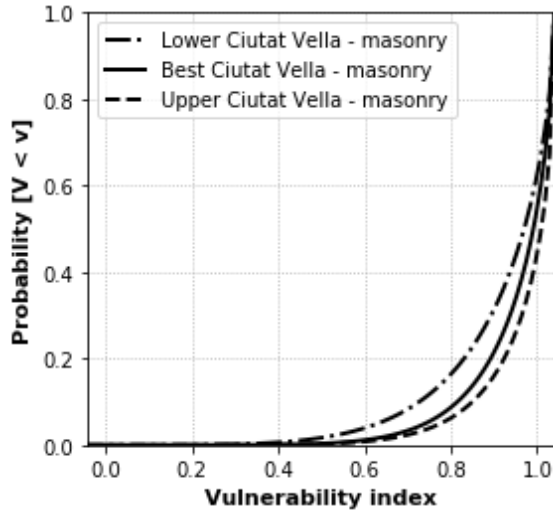
489 At the same time, the additional data to the typology contribute to explain the differences between
490 the levels of seismic vulnerability of the masonry buildings in Ciutat Vella and Nou Barris. Notably,
491 in the case of the studied buildings of Barcelona, the regional modifiers have a significant influence
492 on the final values of seismic vulnerability (Lantada, 2007). These regional modifiers take into
493 account the constructive considerations available in the construction date of the building, and this
494 information is used to infer the probable seismic performance of the buildings (Lantada, 2007).

495 Another factor that explains the average higher levels of seismic vulnerability in the masonry
496 buildings of Ciutat Vella is the fact that in this district, the major part of the masonry buildings
497 (81.1%) corresponds to the M31 structural typology, and in Nou Barris, the major part of the
498 masonry buildings (44.4%) are buildings with M34 structural typology. Therefore, in this case if only
499 the structural typology is considered, the M31 structural typology is more vulnerable than the M34
500 structural typology (Table 6).

501 On the other hand, seismic vulnerability values between the RC buildings in Ciutat Vella (Figure 14b)
502 and Nou Barris (Figure 14d) have a similar magnitude order. For example, according to the *Best*
503 curve, the probability that V is greater than 0.9 is equal to 11.35% and 16.61% for RC buildings in
504 Ciutat Vella and Nou Barris, respectively. In this case, the similitude in the average seismic
505 vulnerability curves of the RC buildings in Ciutat Vella and Nou Barris is mainly due to two conditions:
506 a) the whole RC buildings of both districts are classified into the same structural typology, and b)
507 close of 32% and 34% of the RC buildings in Ciutat Vella and Nou Barris, respectively, were built
508 before 1969. And the structural typology and the construction date are two features that
509 significantly influence the final value of the seismic vulnerability of the buildings.

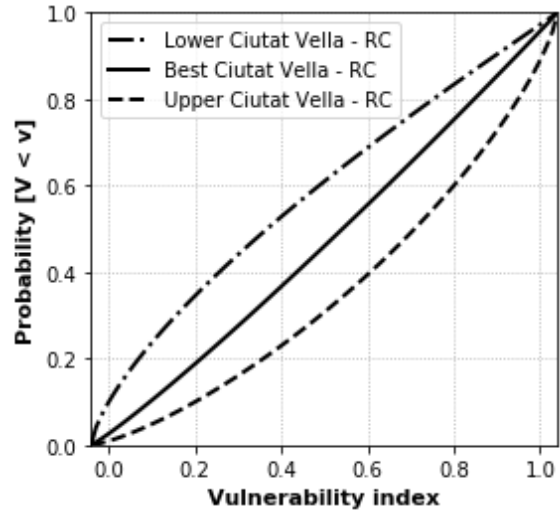
510 We also assessed the vulnerability for subgroups of masonry buildings. For instance, we studied the
511 M31 buildings. We did this analysis because 81.1% of the masonry buildings of Ciutat Vella
512 correspond to this typology (Figure 8). The vulnerability curves computed (Figure 15) show that the
513 M31 buildings in Ciutat Vella (GCV4) have, on average, higher seismic vulnerability than the M31
514 buildings in Nou Barris (GNB4). Notably, the *Best* curve (Figure 15) indicates that the probability that
515 V is greater than 0.9 is equal to 73.80% and 38.69% for M31 buildings in Ciutat Vella (GCV4) and
516 Nou Barris (GNB4), respectively.

517



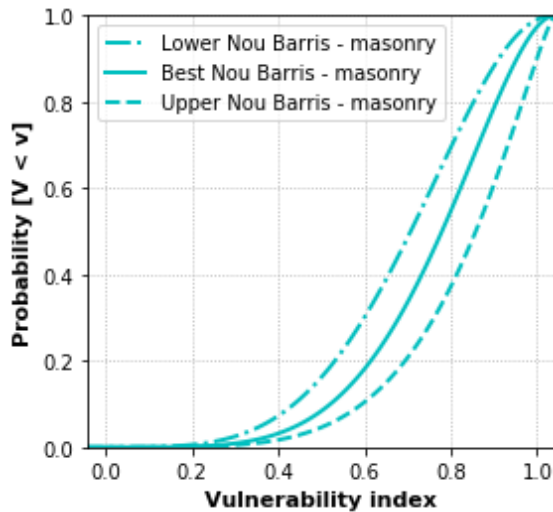
Seismic vulnerability curve	α	β	Mean	SD
Lower	4.64	0.58	0.89	0.14
Best	6.78	0.59	0.92	0.10
Upper	6.66	0.45	0.94	0.09

(a)



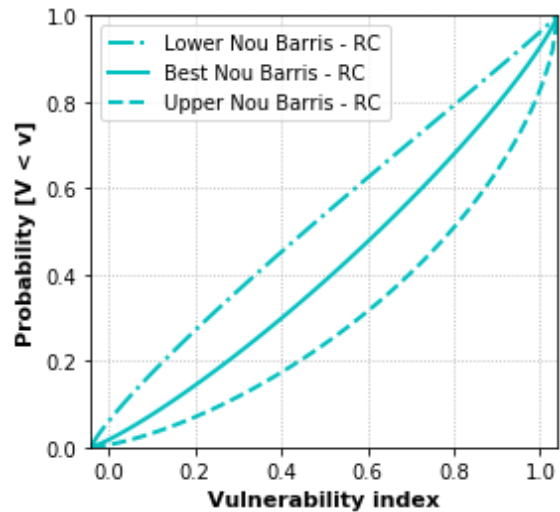
Seismic vulnerability curve	α	β	Mean	SD
Lower	0.70	0.98	0.42	0.32
Best	1.11	0.99	0.53	0.31
Upper	1.32	0.74	0.64	0.30

(b)



Seismic vulnerability curve	α	β	Mean	SD
Lower	4.67	2.26	0.67	0.18
Best	5.32	1.91	0.74	0.17
Upper	5.07	1.27	0.80	0.16

(c)



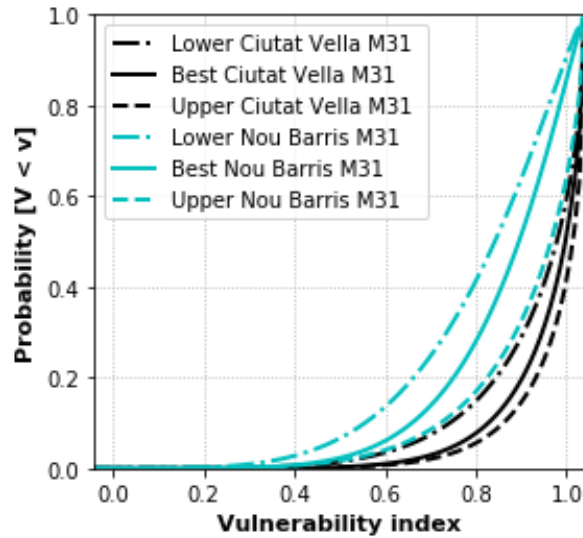
Seismic vulnerability curve	α	β	Mean	SD
Lower	0.84	0.95	0.47	0.32
Best	1.18	0.84	0.58	0.31
Upper	1.41	0.61	0.70	0.29

(d)

518 Figure 14. Seismic vulnerability curves of buildings of masonry (GCV2)(a) and RC (GCV3)(b) in Ciutat Vella and seismic
 519 vulnerability curves of buildings of masonry (GNB2)(c) and RC (GNB3)(d) in Nou Barris. For these cases, it was considered
 520 $V_a = -0.04$ and $V_b = 1.04$.

521 As was mentioned previously, in addition to the structural typology, other features of the buildings
 522 are considered to determine their seismic vulnerability. For this last reason, it is possible to have
 523 cases where buildings of the same structural typology have different levels of seismic vulnerability.

524 Notably, in this case, a significant reason that explains the difference between the average M31
 525 buildings in Ciutat Vella versus the M31 buildings in Nou Barris are the regional vulnerability
 526 modifiers defined by Lantada (2007). According to these modifiers (Table 7), M31 buildings built in
 527 1940 or before have greater vulnerability modifiers than those built after 1940. Moreover, according
 528 to the data, 94.94% and 76.02 % of the M31 buildings in Ciutat Vella and Nou Barris, respectively,
 529 were built in 1940 or before. Therefore, the percentage of M31 buildings in Ciutat Vella that have a
 530 regional modifier for the buildings of 1940 or before is greater than the percentage of the Nou Barris
 531 district that has this feature.



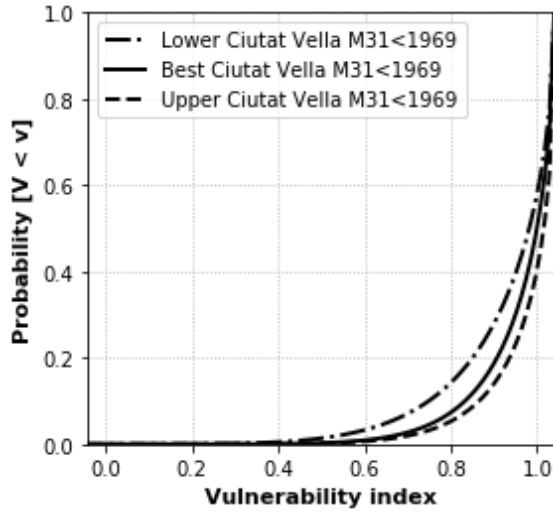
Seismic vulnerability curve	α	β	Mean	SD	Seismic vulnerability curve	α	β	Mean	SD
Lower	4.67	0.54	0.90	0.13	Lower	4.42	1.23	0.78	0.17
Best	6.83	0.55	0.93	0.10	Best	5.89	1.17	0.83	0.14
Upper	6.74	0.42	0.94	0.09	Upper	4.72	0.61	0.89	0.14

Ciutat Vella

Nou Barris

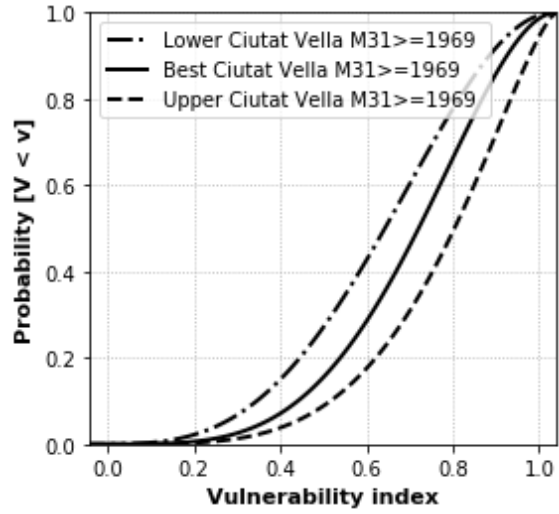
532 Figure 15. Seismic vulnerability curves for the masonry M31 buildings in Ciutat Vella (GCV4) and Nou Barris (GNB4)
 533 considering $V_a=-0.04$ and $V_b=1.04$.

534 Additionally, we analyzed two subgroups of the M31 buildings of each district, considering the
 535 variable of the year of construction. For this analysis, we choose the 1969 year as the reference
 536 point because Barcelona's first seismic code was used in that year (Lantada 2007). The results
 537 (Figure 16) indicate that the M31 buildings built during or after 1969 in Ciutat Vella (GCV6) and Nou
 538 Barris (GNB6) have, on average, a significantly lower seismic vulnerability than the M31 buildings
 539 built before that year. Moreover, if we analyze the Best vulnerability curves (Figure 16), we can
 540 verify additional conclusions. For instance, in this last case, we can observe that the probability that
 541 V is greater than 0.8 is equal to 90.79% and 28.8% for the M31 buildings in Ciutat Vella built before
 542 1969 (GCV5) (Figure 16a) and during or after 1969 (GCV6) (Figure 16b), respectively. We also
 543 observed that, on average, the M31 buildings that were built during or after 1969 in Ciutat Vella
 544 (GCV6) (Figure 16b) have higher levels of seismic vulnerability than the buildings that were also built
 545 during or after 1969 in Nou Barris (GNB6) (Figure 16d). For instance, the Best vulnerability curve
 546 shows that the probability that V is greater than 0.8 is equal to 28.8% and 20.9% for the M31
 547 buildings built during or after 1969 in Ciutat Vella (GCV6) (Figure 16b) and Nou Barris (GNB6) (Figure
 548 16d), respectively.



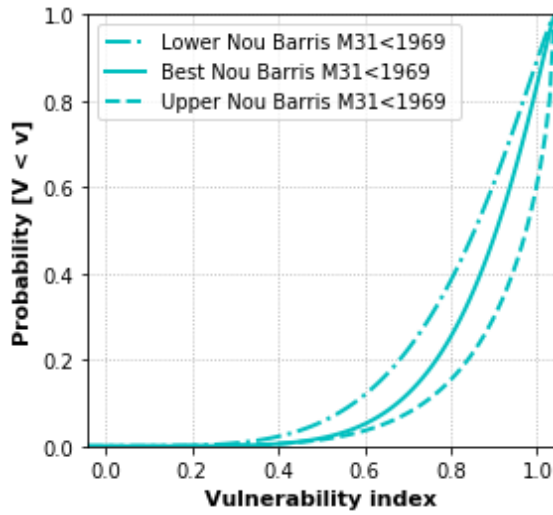
Seismic vulnerability curve	α	β	Mean	SD
Lower	4.69	0.52	0.90	0.13
Best	6.89	0.53	0.93	0.10
Upper	6.79	0.41	0.94	0.09

(a)



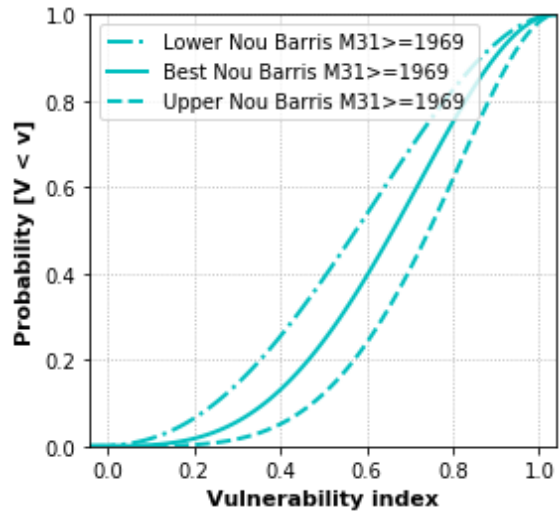
Seismic vulnerability curve	α	β	Mean	SD
Lower	3.56	2.20	0.62	0.20
Best	4.42	2.04	0.68	0.18
Upper	4.41	1.46	0.75	0.18

(b)



Seismic vulnerability curve	α	β	Mean	SD
Lower	4.58	1.19	0.79	0.17
Best	6.08	1.13	0.84	0.14
Upper	4.71	0.56	0.89	0.13

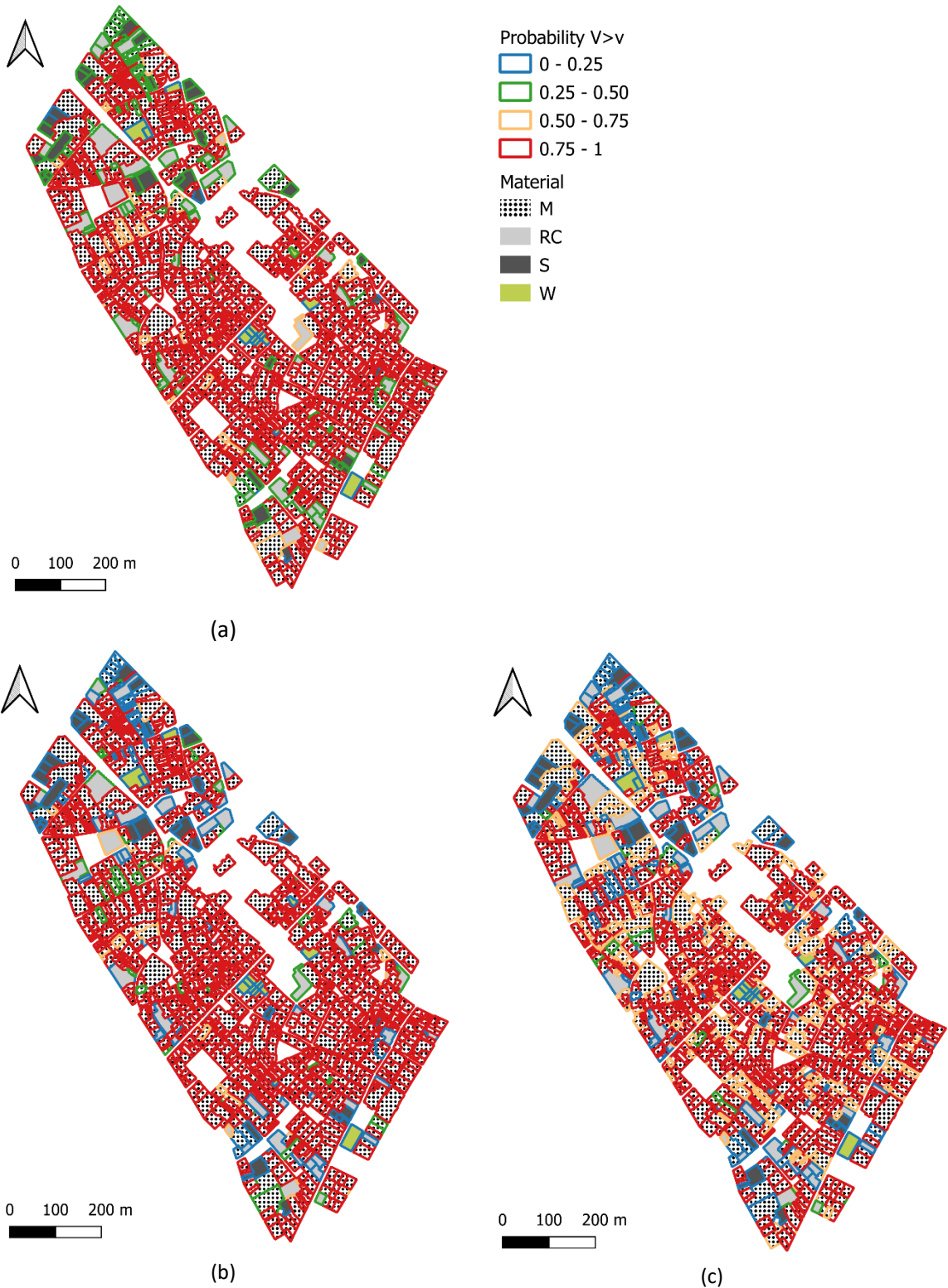
(c)



Seismic vulnerability curve	α	β	Mean	SD
Lower	2.55	2.00	0.56	0.23
Best	3.67	2.12	0.63	0.20
Upper	4.84	2.01	0.71	0.18

(d)

550 Figure 16. Seismic vulnerability curves for the masonry M31 buildings built before 1969 (GCV5) (a) and during or after 1969
 551 (GCV6) (b) in Ciutat Vella (top) and the seismic vulnerability curves for the masonry M31 buildings built before 1969 (GNB5)
 552 (c) and during or after 1969 (GNB6) (d) in Nou Barris considering $V_a=-0.04$ and $V_b=1.04$.



554 Figure 17. Maps of seismic vulnerability of residential buildings in the Gothic neighborhood of the Ciutat Vella district, in
 555 terms of the probability that V is greater than 0.7(a), 0.8(b), and 0.9(c) considering the Best vulnerability functions.

556 The computed seismic vulnerability curves can also be used to generate seismic vulnerability maps
 557 like the ones included in Figure 17. The data of the map of Figure 17a allows identifying that 85.36%
 558 of residential buildings in the Gothic neighborhood of Ciutat Vella have a probability superior to 0.75
 559 that V is greater than 0.7 (if the *Best* vulnerability curves are considered). The Ciutat Vella district is
 560 divided into four neighborhoods: i) Raval; ii) Gothic; iii) Barceloneta, and iv) Santa Pere, Santa
 561 Caterina i la Ribera (Ajuntament de Barcelona, 2020). Similarly, the results represented in the maps
 562 of Figure 17b and Figure 17c indicate that 84.44% and 66.36% of residential buildings in the Gothic
 563 neighborhood of Ciutat Vella have a probability superior to 0.75 that V is greater than 0.8 and 0.9,
 564 respectively (if the *Best* vulnerability curves are considered). In contrast, the results in the Nou Barris
 565 district's case show that 24.29% of dwelling buildings of this district have a probability superior to
 566 0.75 that V is greater than 0.7. Similarly, 17.31% and 0.51% of residential buildings in Nou Barris
 567 have a probability superior to 0.75 that V is greater than 0.8 and 0.9, respectively (considering the
 568 *Best* vulnerability curves).

569

570 2.5. Seismic Risk of Ciutat Vella and Nou Barris

571

572 According to the VIM_P, Eq. (6) was applied to compute the seismic risk of the studied buildings.
 573 Particularly, the seismic risk of each building was computed considering their respective seismic
 574 hazard curves and the seismic vulnerability functions of the studied building. For instance, applying
 575 USERISK2015, the seismic risk results of the buildings included in Table 8 were computed. For this
 576 case, the seismic hazard curves used are the curves of black lines in Figure 5. These curves were
 577 truncated to 475 years and the vulnerability functions considered are included in Figure 10. Table
 578 13 and Figure 18 shows the computed seismic risk results. These last results correspond to the
 579 seismic risk for each one of the four studied buildings. However, it is also possible to use these
 580 seismic risk results to obtain the risk for a group of buildings as it was described by Aguilar-Meléndez
 581 et al. (2019a). Figure 19 shows the case of the seismic risk results determined for a group of the two
 582 buildings: CV1 and CV2.

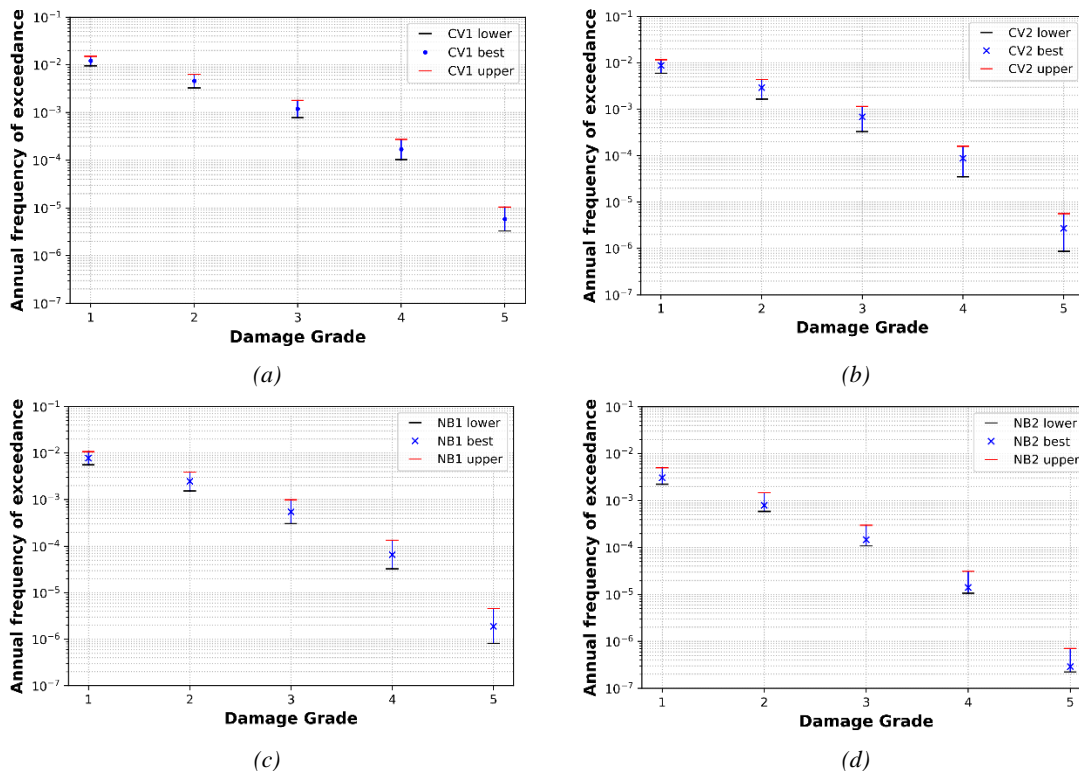
583

584 *Table 13. Results of Seismic risk of buildings CV1, CV2, NB1, and NB2 in Barcelona in terms of the average of the annual*
 585 *frequency of exceedance of the damage grades (1-5) computed considering a seismic hazard truncated to 475 years*

Building	VC	v (D) [1/years]				
		D1	D2	D3	D4	D5
CV1	L	9.5E-3	3.28E-3	7.9E-4	1.03E-4	3.29E-6
	B	1.21E-2	4.61E-3	1.2E-3	1.69E-4	5.91E-6
	U	1.51E-2	6.35E-3	1.8E-3	2.73E-4	1.04E-5
CV2	L	5.99E-3	1.66E-3	3.3E-4	3.51E-5	8.73E-7
	B	8.79E-3	2.94E-3	6.91E-4	8.78E-5	2.73E-6
	U	1.17E-2	4.43E-3	1.15E-3	1.61E-4	5.61E-6
NB1	L	5.59E-3	1.54E-3	3.06E-4	3.26E-5	8.18E-7
	B	7.83E-3	2.46E-3	5.46E-4	6.54E-5	1.89E-6
	U	1.07E-2	3.92E-3	9.91E-4	1.35E-4	4.56E-6
NB2	L	2.24E-3	5.85E-4	1.09E-4	1.07E-5	2.23E-7
	B	3.06E-3	7.94E-4	1.47E-4	1.41E-5	2.89E-7
	U	5.05E-3	1.47E-3	2.98E-4	3.12E-5	7.05E-7

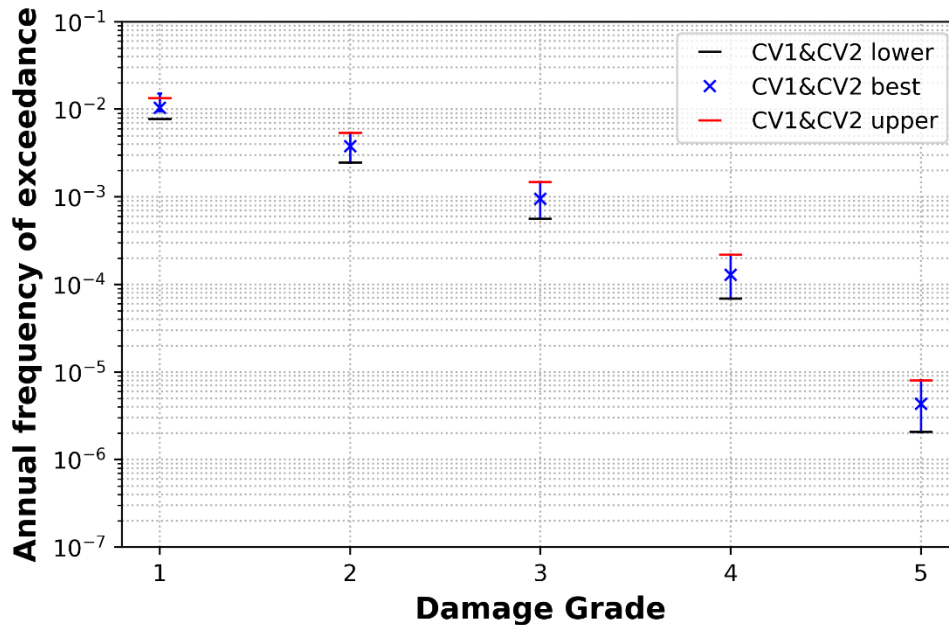
586 If we consider the individual seismic risk, it is possible to observe that in the CV1 building, the annual
 587 frequency of exceedance of the collapse damage state ranges between 3.29×10^{-6} and 1.04×10^{-5} , with
 588 a mean value of 5.91×10^{-6} . Similarly, in the CV2 building, the annual frequency of exceedance of the
 589 collapse damage state ranges between 8.73×10^{-7} and 5.61×10^{-6} , with a mean value of 2.73×10^{-6} . On
 590 the other hand, if we consider the mean values, we can affirm that the CV1 building has twice the
 591 seismic risk of the CV2 building. At the same time, it is possible to highlight that if the upper value is
 592 considered, we can observe that the seismic risk of the CV1 building exceeds the value of 1×10^{-5} .
 593 Therefore, if a decision criterion states that the building with a higher level of seismic risk greater
 594 than 1×10^{-5} (Stirrat and Jury, 2017; Hardy et al., 2017) must require an additional detailed revision,
 595 then the building CV1 would require this kind of revision.

596
 597 In this study, we applied USERISK2015 (Aguilar-Meléndez et al. 2016) to compute the seismic risk of
 598 Ciutat Vella and Nou Barris's residential buildings. First, we computed seismic risk applying the
 599 seismic hazard curves determined in the present work (Figure 5) truncated to 475 years (10%
 600 probability of exceedance in 50 years). Additionally, we computed seismic risk considering the same
 601 hazard curves but truncated to 975 years (5% probability of exceedance in 50 years). We computed
 602 the seismic risk for seismic hazard for these two return periods (475 and 975 years) because, as a
 603 part of the seismic risk management, it is convenient to have results of seismic risk for different
 604 return periods of seismic hazard to facilitate the stakeholders the decision procedures. Even though
 605 the return periods selected are common values to compute seismic hazard (Solomos et al., 2008),
 606 they are not unique options. For this reason, the VIM_P allows computing the seismic risk for the
 607 diverse return periods that could be necessary.
 608



609 Figure 18. Seismic risk of buildings CV1(a), CV2(b), NB1(c), and NB2(d) in Barcelona in terms of the average of the annual
 610 frequency of exceedance of the damage grades (1-5) computed considering a seismic hazard truncated to 475 years

611 For the first case (475 years), the seismic risk computed of Ciutat Vella and Nou Barris’s residential
 612 buildings is shown in Figure 20. Specifically, according to Figure 20, on average, the seismic risk of
 613 the residential buildings of Ciutat Vella is higher than the seismic risk of the residential buildings of
 614 Nou Barris. For instance, if we observe the results obtained using the *Best* vulnerability curves
 615 (Figure 20), we can identify that the damage grade 5 (total collapse) has an annual frequency of
 616 exceedance equal to 1.46×10^{-5} and 3.14×10^{-6} for the residential buildings of Ciutat Vella and Nou
 617 Barris, respectively. These results agree with Lantada et al. (2010) study because they also
 618 concluded that the seismic risk in Ciutat Vella is significantly higher than in Nou Barris.
 619

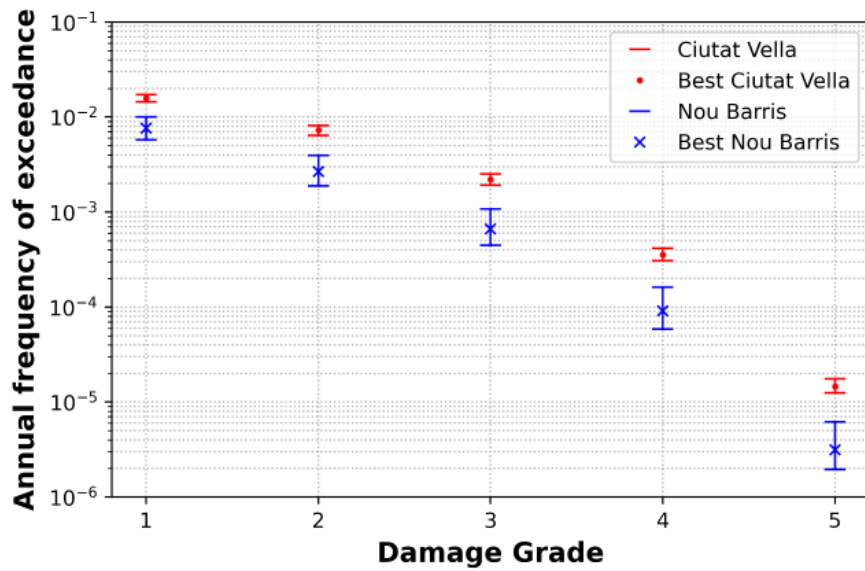


620
 621 *Figure 19. Average risk of buildings CV1 and CV2 in Barcelona in terms of the average of the annual frequency of*
 622 *exceedance of the damage grades (1-5) computed considering a seismic hazard truncated to 475 years*

623
 624 Additionally, the results show that 70.04%, 70.31%, and 82.26% of the Buildings in Ciutat Vella
 625 (GCV1) have an exceedance frequency of the collapse damage state greater than 1×10^{-5} , if the
 626 *Lower*, *Best*, and *Upper* vulnerability curves are considered, respectively. Similarly, 1.06%, 2.81%,
 627 and 28.11% of the Buildings in Nou Barris (GNB1) have an exceedance frequency of the collapse
 628 damage state greater than 1×10^{-5} , if the *Lower*, *Best*, and *Upper* vulnerability curves are considered,
 629 respectively.

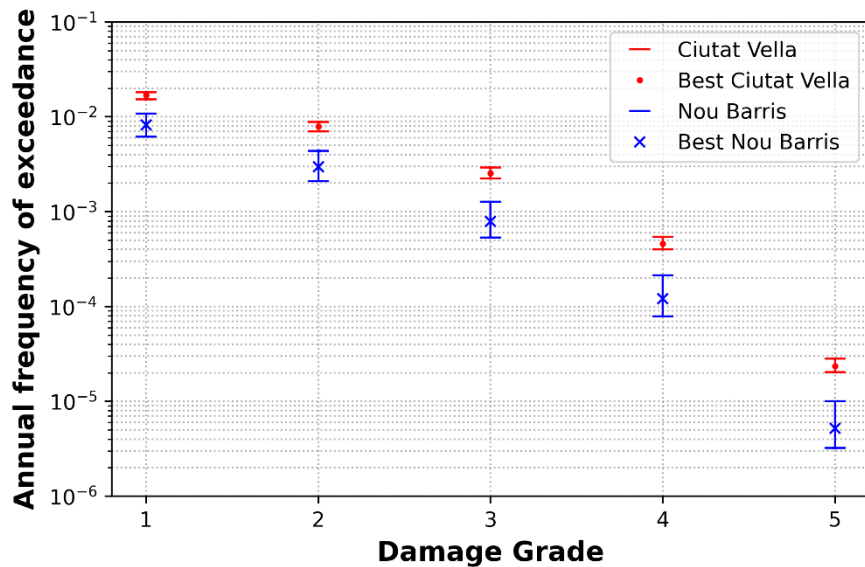
630
 631 On the other hand, Figure 21 shows seismic risk results computed using seismic hazard truncated to
 632 975 years. These risk results indicate that the damage grade 5 (total collapse) has an annual
 633 frequency of exceedance equal to 2.35×10^{-5} and 5.17×10^{-6} for Ciutat Vella (GCV1) and Nou Barris
 634 (GNB1) buildings, respectively. Therefore, analyzing these previous results, we can affirm that the
 635 seismic risk related to the damage grade 5 in both districts increases by about 70% when we modify
 636 the truncation limit of the seismic hazard from 475 years to 975 years. The same seismic risk results
 637 indicate that 81.07% and 23.02% of the buildings in Ciutat Vella and Nou Barris, respectively, have
 638 an exceedance frequency of the collapse damage state greater than 1×10^{-5} , if the *Best* vulnerability
 639 curve and the seismic hazard of 975 years are considered.

640



641 *Figure 20. Seismic risk of Ciutat Vella (GCV1) and Nou Barris (GNB1) in Barcelona in terms of the average of the annual*
642 *frequency of exceedance of the damage grades (1-5) computed considering a seismic hazard truncated to 475 years.*

643



644 *Figure 21. Seismic risk of Ciutat Vella (GCV1) and Nou Barris (GNB1) in Barcelona in terms of the average of the annual*
645 *frequency of exceedance of the damage grades (1-5) computed considering a seismic hazard truncated to 975 years.*

646 Additionally, Figure 22 shows another way to communicate the seismic risk computed according to
647 the VIM_P. Particularly, in this figure, we can observe maps that display the location and shape of
648 each plot where a residential building exists in the Gothic neighborhood of the Ciutat Vella District.
649 However, at the same time, these maps show the seismic risk of the building located in each plot in
650 terms of the annual frequency of exceedance of the damage grade 5. Moreover, these maps display
651 the main structural material of each studied building.

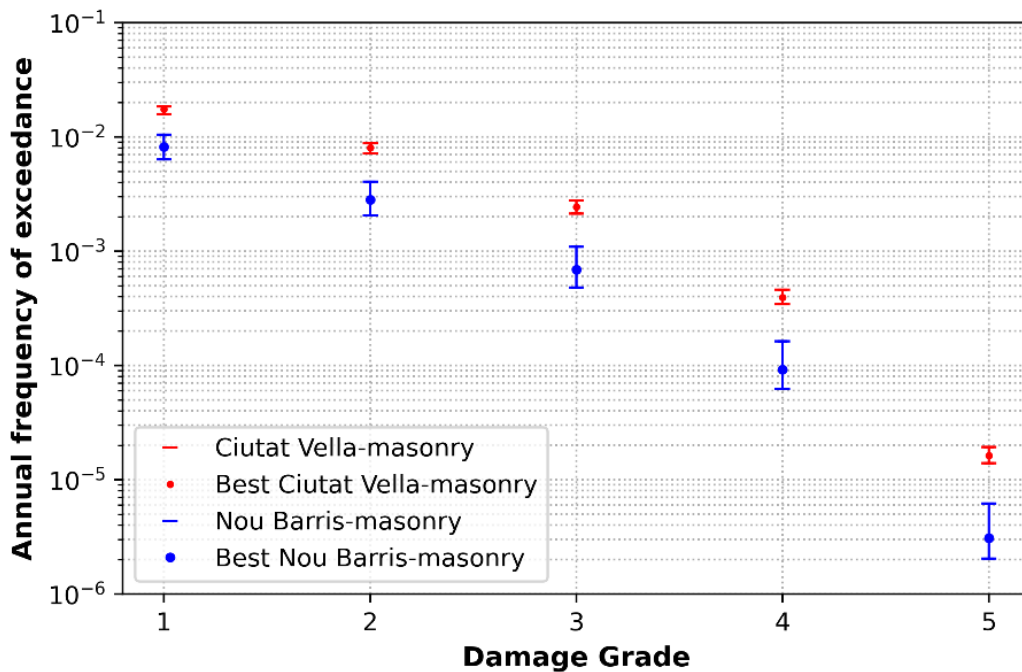
652 According to the seismic results of Figure 22, the percentage of dwelling buildings in the Gothic
 653 neighborhood that has a frequency of occurrence of damage five greater than 1×10^{-5} is 70.42%,
 654 70.57%, and 77.93%, respectively, when the *Lower*, *Best*, and *Upper* vulnerability curves are
 655 considered.

656



657 *Figure 22. Seismic risk maps of the Gothic neighborhood of Ciutat Vella to cadastral plot scale. These maps show the seismic*
 658 *risk and the main structural material of each residential building of the Gothic neighborhood of Ciutat Vella. The seismic*
 659 *risk is in terms of annual frequency of damage D5, and this risk was obtained considering a seismic hazard curve truncated*
 660 *to 475 years and the Lower (a), Best (b), and Upper (c) seismic vulnerabilities curves.*

661 As stated in Figure 23, the average seismic risk of the masonry buildings in Ciutat Vella is higher than
 662 the average seismic risk of the masonry buildings in Nou Barris. For instance, according to the *Best*
 663 vulnerability curve (Figure 23), the annual frequency of exceedance of damage 5 in the masonry
 664 buildings is equal to 1.62×10^{-5} and 3.08×10^{-6} in Ciutat Vella (GCV2) and Nou Barris (GNB2),
 665 respectively. These values also mean that the seismic risk of the masonry buildings in Ciutat Vella is
 666 5.3 times higher than the seismic risk of the masonry buildings in Nou Barris. Similarly, we can
 667 observe that considering the *Best* vulnerability curves (Figure 24a and Figure 24b), the annual
 668 frequency of exceedance of the damage 5 in the reinforced concrete buildings is equal to 2.35×10^{-6}
 669 and 3.53×10^{-6} in Ciutat Vella (GCV3) and Nou Barris (GNB3), respectively. Therefore, in this case,
 670 the average seismic risk of the reinforced concrete buildings is 1.5 times higher in Nou Barris than
 671 in Ciutat Vella.

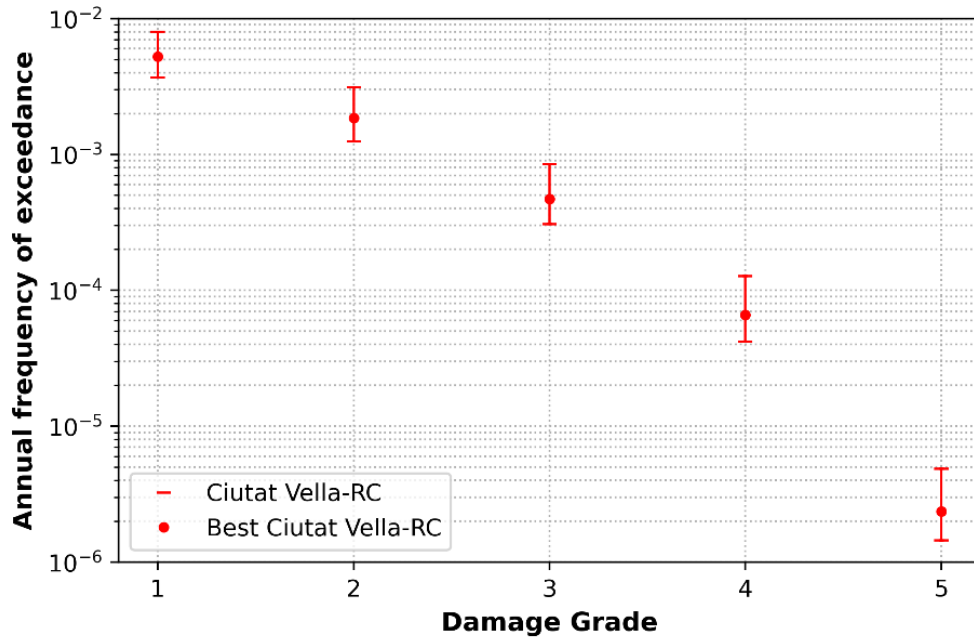


672 *Figure 23. Seismic risk of masonry buildings of Ciutat Vella (GCV2) and Nou Barris (GNB2) in terms of the average of the*
 673 *annual frequency of exceedance of the damage grades (1-5), computed considering a seismic hazard truncated to 475*
 674 *years.*

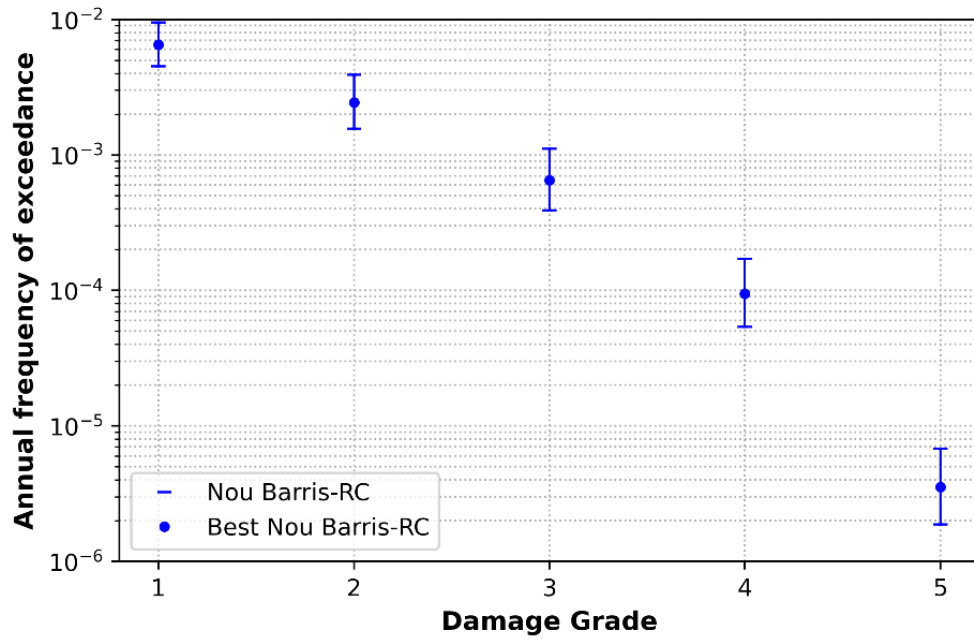
675

676 It can be observed that buildings in Ciutat Vella with six or more stories (GCV8) have, on average,
 677 higher seismic risk than buildings with five or fewer stories (GCV7) (Table 14). For instance, for the
 678 best vulnerability curve, the average seismic risk for the damage grade 5 is equal to 1.1×10^{-5} and
 679 1.64×10^{-5} for buildings with five or fewer stories and six or more stories, respectively.

680 Similarly, Table 14 shows that buildings in Nou Barris with six or more stories (GNB8) have, on
 681 average, higher seismic risk than buildings with five or fewer stories (GNB7). For example, the best
 682 vulnerability curve indicates that the average seismic risk for the damage grade 5 is equal to
 683 2.96×10^{-6} and 3.55×10^{-6} for buildings in Nou Barris with five or fewer stories and six or more stories,
 684 respectively.



(a)



(b)

686 Figure 24. Seismic risk of reinforced concrete buildings of Ciutat Vella (GCV3) (a) and seismic risk of reinforced concrete
 687 buildings of Nou Barris (GNB3) (b). The seismic risk is in terms of the average of the annual frequency of exceedance of the
 688 damage grades (1-5), computed considering a seismic hazard truncated to 475 years.

689

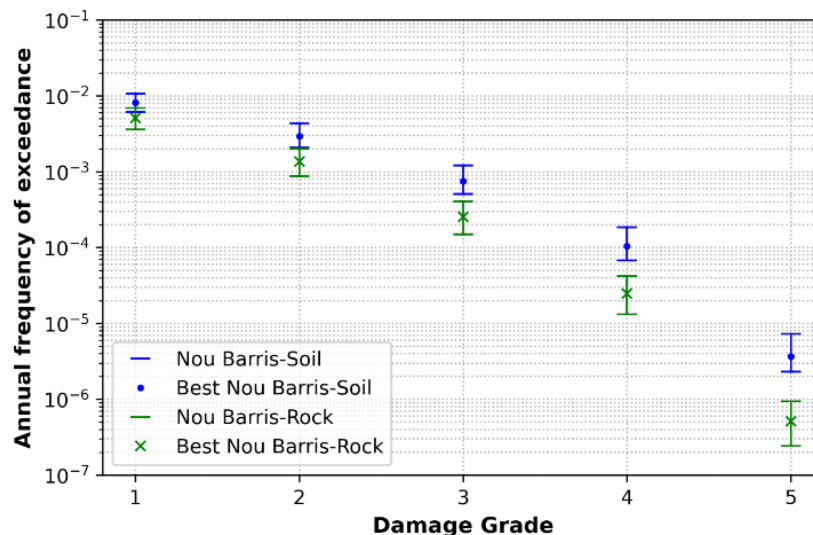
690

691 Table 14. Seismic risk for the buildings in Ciutat Vella (left) and Nou Barris (right) considering two groups of buildings: I)
 692 buildings with five or fewer stories and II) buildings with six or more stories. These results were computed considering a
 693 seismic hazard truncated to 475 years and the Best vulnerability curve of the buildings (Figure 9).

District	Buildings	VC	v (D) [1/years]				
			D1	D2	D3	D4	D5
Ciutat Vella	Residential buildings with five or fewer stories (GCV7)	L	1.72E-02	7.97E-03	2.43E-03	3.96E-04	1.64E-05
		B	1.47E-02	6.36E-03	1.83E-03	2.83E-04	1.10E-05
		U	1.68E-02	7.84E-03	2.41E-03	3.95E-04	1.65E-05
	Residential buildings with six or more stories (GCV8)	L	1.51E-02	6.94E-03	2.11E-03	3.44E-04	1.43E-05
		B	1.66E-02	7.73E-03	2.38E-03	3.91E-04	1.64E-05
		U	1.74E-02	8.27E-03	2.58E-03	4.28E-04	1.81E-05
Nou Barris	Residential buildings with five or fewer stories (GNB7)	L	5.88E-03	1.93E-03	4.58E-04	6.01E-05	1.99E-06
		B	7.59E-03	2.63E-03	6.48E-04	8.74E-05	2.96E-06
		U	9.88E-03	3.82E-03	1.04E-03	1.54E-04	5.88E-06
	Residential buildings with six or more stories (GNB8)	L	5.46E-03	1.78E-03	4.22E-04	5.57E-05	1.86E-06
		B	7.65E-03	2.75E-03	7.04E-04	9.92E-05	3.55E-06
		U	1.05E-02	4.21E-03	1.17E-03	1.78E-04	6.90E-06

694 VC=vulnerability curve; L=Lower; B=Best; U=Upper

695 Additionally, we compared the seismic risk of buildings of Nou Barris founded on soil and rock.
 696 Figure 25 displays that buildings of Nou Barris founded on soil have, on average, a seismic risk higher
 697 than the seismic risk of buildings of Nou Barris founded on rock. For instance, for damage grade 5,
 698 the annual frequency of exceedance is equal to 5.11×10^{-7} and 3.68×10^{-6} for buildings on rock and
 699 soil, respectively. According to these results, the seismic risk of the Nou Barris buildings founded on
 700 soil is, on average, 7.2 times greater than the seismic risk of the buildings of the same district
 701 founded on rock.



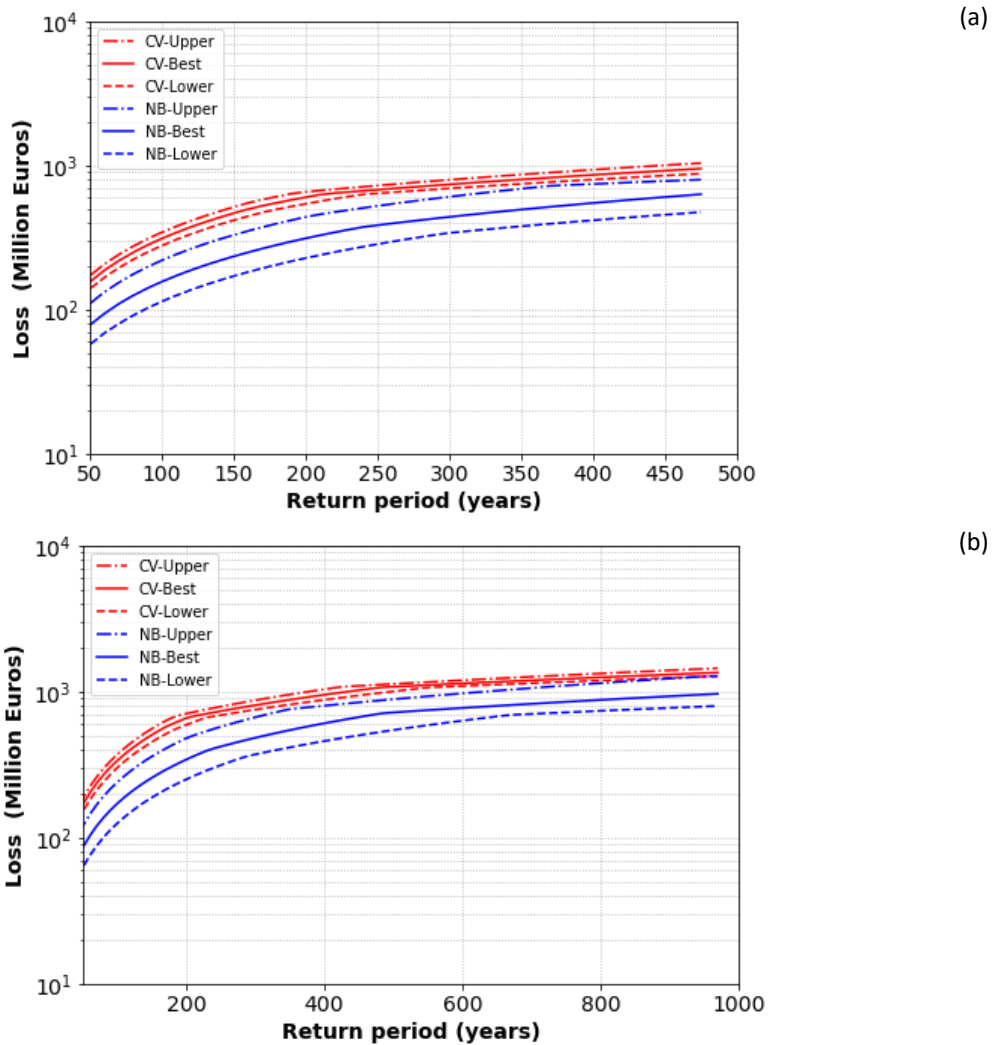
702 Figure 25. Seismic risk of the buildings in Nou Barris on soil and rock computed considering a seismic hazard truncated to
 703 475 years
 704

705 2.6. Seismic risk in economic terms

706 We used the seismic risk results in terms of physical damage (Figure 21a) to assess economic losses.
 707 For this purpose, we considered that according to Marulanda et al. (2013), €31523 million is the

708 overall value of Barcelona’s total residential buildings. Additionally, we applied the proposal that
 709 states that the economic cost factors are equal to 0.035, 0.145, 0.305, 0.800, and 1.00 for the
 710 occurrence of damage states 1,2,3,4, and 5, respectively (Dolce et al. 2006).

711 The economic cost obtained by Lantada et al. (2018) for Ciutat Vella shows good agreement with
 712 the losses computed in the present study. Particularly, Lantada et al. (2018) computed €591 and
 713 €1105 million of economical cost in Ciutat Vella due to a seismic event of intensity VI and VI-VII,
 714 respectively. The losses of €1105 million also correspond to a probabilistic seismic scenario with a
 715 return period of 475 years. In this study, the economic losses related to a return period of 475 years
 716 are equal to €875.65, €948.55, and €1037.06 million for the *Low*, *Best*, and *Upper* cases, respectively
 717 (Figure 26a). Similarly, the economic losses that we computed for Nou Barris are equal to €473.13,
 718 €630.12, and €795.97 million for the *Low*, *Best*, and *Upper* case, respectively (Figure 26b). Moreover,
 719 the economic losses for the *Best* case are equal to €1349.39 and €965.43 for Ciutat Vella and Nou
 720 Barris, respectively (Figure 26b) if a return period of 975 years is considered.



721 Figure 26. Seismic risk curves of the residential buildings of Ciutat Vella and Nou Barris in terms of economic losses versus
 722 return periods. These curves were obtained considering the seismic hazard curves computed in the present work (Figure 5)
 723 truncated to 475 years (a) and 975 years (b).

724 3. Discussion and conclusions

725

726 The VIM_P is a versatile methodology to assess seismic vulnerability and the seismic risk of
727 residential buildings. Specifically, in this study, we analyzed the residential buildings of Ciutat Vella
728 and Nou Barris districts in Barcelona. Both seismic vulnerability and seismic risk results obtained
729 with this methodology are valuable information that could be used to make essential decisions
730 oriented to increase seismic resilience in cities.

731 ***Seismic hazard***

732 The seismic hazard curve computed for Barcelona agrees with previous seismic hazard assessments.
733 For instance, based on the results (Figure 5), the intensity with a return period of 475 years for a
734 rock site is slightly less than the macroseismic grade VI. This last result agrees with the intensity of
735 VI determined by the IGN (2017) for Barcelona for a return period of 475 years. We highlighted that
736 the Lorca earthquake in 2011 generated substantial damage (Aguilar-Meléndez et al. 2019c), and
737 this disaster contributed to increasing the interest in performing new assessments of the seismic
738 hazard of Spain.

739 ***Vulnerability***

740 The results show that the buildings in Ciutat Vella have, on average, significantly higher seismic
741 vulnerability than the buildings in Nou Barris. For instance, if we consider the *Best* vulnerability
742 curve, then the probability that a building has a vulnerability index greater than 0.8 could be 83.59%
743 and 34.03% in Ciutat Vella and Nou Barris, respectively. The results also indicate that in Ciutat Vella,
744 the buildings with six or more stories are, on average, more vulnerable than buildings with five or
745 fewer stories. For example, in this district, the probability that V is greater than 0.9 is equal to
746 51.89% and 68.17% (*Best*-curve-Table 12) for buildings with fewer than six stories and more than
747 five stories, respectively. However, in Nou Barris's case, the seismic vulnerability between buildings
748 with six or more stories and buildings with five or fewer stories have fewer differences than in the
749 case of Ciutat Vella's buildings. Specifically, when we analyzed a level of seismic vulnerability
750 represented by $V > 0.7$, then the buildings in Nou Barris with fewer than six stories have more
751 probability (55.28%-Table 12) of exceeding that level of vulnerability than the buildings with more
752 than five stories (50.41%-Table 12). However, if we analyze a level of vulnerability represented by
753 $V > 0.9$, then the buildings in Nou Barris with more than five stories have more probability (15.66%-
754 Table 12) of exceeding that level of vulnerability than the buildings with fewer than six stories
755 (13.15%-Table 12).

756 It is essential to highlight that even though, on average, the masonry buildings in Ciutat Vella have
757 higher levels of seismic vulnerability than the masonry buildings in Nou Barris, in the case of the RC
758 buildings, this behavior is not the same. Conversely, the RC buildings in Nou Barris are slightly more
759 vulnerable than the RC buildings in Ciutat Vella. These differences are mainly related to the age of
760 the buildings because this age is used to determine the design procedures that were considered to
761 design each building. And this feature is considered in the regional modifiers for the Barcelona'
762 buildings (Table 7) that were defined by Lantada (2007). Notably, on average, the masonry buildings
763 in Ciutat Vella are older than the masonry buildings in Nou Barris. On the other hand, on average,
764 the RC buildings in Nou Barris are slightly older than the RC buildings in Ciutat Vella. For instance, if

765 we consider the *Best* curve, the probability that V is greater than 0.9 is equal to 16.61 % and 11.35%
766 for the RC buildings in Nou Barris and Ciutat Vella, respectively.

767 We also analyzed the case of the masonry buildings M31, and the results show that the M31
768 buildings in Ciutat Vella are, on average, more vulnerable than the same type of buildings in Nou
769 Barris. This last condition is because not only the structural typology is considered to determine the
770 seismic vulnerability of the buildings, and, in this case, the regional modifiers have a significant
771 influence on the final values of seismic vulnerability of each studied building (Table 7).

772 On the other hand, a year that has been associated with a relevant reduction in the seismic
773 vulnerability of buildings in Barcelona is 1969. This last condition is because, during this year, the
774 first seismic code in the city was applied. For this last reason, even the M31 buildings in Ciutat Vella
775 have significant differences in their seismic vulnerability depending on the year of construction. For
776 instance, if we consider the best vulnerability curve, then the probability that V is greater than 0.8
777 is equal to 90.79% for M31-buildings in Ciutat Vella built before 1969 and equal to 28.8% for the
778 M31-buildings built in the same district during or after 1969.

779 The seismic vulnerability can also be communicated through vulnerability maps like the ones shown
780 in Figure 17 to help a broader range of stakeholders. These maps show the different levels of seismic
781 vulnerability of the buildings in the Gothic neighborhood of Ciutat Vella.

782 **Risk**

783 The results show that if the *Best* vulnerability curve and a seismic hazard curve truncated to 475
784 years are considered, then 70.31% and 2.81% of the buildings in Ciutat Vella and Nou Barris,
785 respectively, have an exceedance frequency of the collapse damage state greater than 1×10^{-5} .
786 Therefore, if we consider this last value as the limit of acceptable seismic risk, then it can be
787 observed that the major part (70.31%) of Ciutat Vella's buildings could have a not acceptable level
788 of seismic risk. Consequently, this district could be considered a Barcelona region where the
789 buildings require a special program to verify their structural safety, including their appropriate
790 behavior during earthquakes. On the other hand, in Nou Barris, the percentage of buildings that
791 exceed the reference seismic risk level is 2.81%. Therefore, in this case, it could be convenient to
792 verify the buildings' structural safety with the emphasis on the buildings that exceed the reference
793 level of seismic risk previously mentioned.

794 It should be noted that the results show that not all the buildings in Ciutat Vella have more seismic
795 risk than the buildings in Nou Barris. Specifically, the RC buildings of Nou Barris have, on average, a
796 seismic risk level 1.5 times greater than the RC buildings of Ciutat Vella if the *Best* curve is
797 considered. Simultaneously, it is convenient to notice that according to the results (Figure 25), the
798 buildings of Nou Barris in soil have, on average, a seismic risk level 7 times greater than the buildings
799 of the same district located in rock.

800 The seismic risk maps of Figure 22 are an option to communicate the residential buildings' seismic
801 risk to the stakeholders. This information could be used to make decisions that increase the seismic
802 resilience of the cities. It is essential to highlight that the VIM_P allows assessing the seismic risk in
803 terms of annual frequency of exceedance of damage states, which does not occur with the VIM
804 antecedent method. At the same time, the VIM_P allows computing the seismic risk in terms of
805 losses with different return periods. This last type of information is, for instance, relevant for the

806 insurance industry. Therefore, the appropriate application of the VIM_P can contribute to
807 generating valuable information for the different stakeholders related to the management of the
808 seismic risk of buildings in urban areas.

809 ***Comparison with previous results***

810 The losses assessed in the present study for Ciutat Vella agree with the losses obtained by Lantada
811 et al., 2018. They assessed losses of €1105 million for a seismic scenario associated with a return
812 period of 475 years, and we estimated losses of €948.55 million for a return period of 475 years. In
813 this aspect, it is convenient to underline that the comparison focuses on the order of magnitude of
814 the economic losses because the methodology used to compute the losses by Lantada et al. (2018)
815 was the VIM, and in the present study, we applied the VIM_P. As was mentioned by Aguilar-
816 Meléndez et al. (2019a), the type of seismic results that can be obtained by each one of these two
817 methods are not the same. On the other hand, the seismic vulnerability results obtained in the
818 present study for the masonry and RC buildings in Ciutat Vella agree with the results determined by
819 Lantada et al. 2018, because they also computed significant differences between the seismic
820 vulnerability of both groups of buildings of the Ciutat Vella district.

821 **Acknowledgments**

822 The present research has received partial funding from the European Union's Horizon 2020 research
823 and innovation program (grant agreement N° 823844, ChEESA CoE Project).

824 **Declarations**

825 **Funding**

826 The present research has received partial funding from the European Union's Horizon 2020 research
827 and innovation program (grant agreement N° 823844, ChEESA CoE Project).

828 **Conflicts of interest/Competing interests**

829 The authors declare that there is no conflict of interest.

830 **Availability of data and material**

831 The database generated during and analyzed during the current study is not publicly available due
832 to the sensitivity of the data of the buildings.

833 **Code availability**

834 R-CRISIS code can be downloaded at the site <http://www.r-crisis.com/> and USERISK2015 can be
835 requested at the site <https://sites.google.com/site/userisk2015/>

836

837 **Ethics approval**

838 We declare that we do not have any commercial or associative interest that represents a conflict
839 of interest in connection with the work submitted.

840 **Consent to participate**

841 Not applicable

842 **Consent for publication**

843 Not applicable

844 **References**

845 Ademović N, Hadzima-Nyarko M & Zagora N (2020). Seismic vulnerability assessment of masonry
846 buildings in Banja Luka and Sarajevo (Bosnia and Herzegovina) using the macroseismic model.
847 Bull Earthquake Eng 18, 3897–3933. <https://doi.org/10.1007/s10518-020-00846-8>

848 Aguilar-Meléndez A (2011). Evaluación probabilista del riesgo sísmico de edificios en zonas urbanas.
849 Tesis doctoral. Universidad Politécnica de Cataluña, 297 pp.
850 <https://www.tdx.cat/handle/10803/668388>

851 Aguilar-Meléndez, A, Pujades, LG, Barbat, AH, Ordaz, MG, de la Puente, J, Lantada, N, & Rodríguez-
852 Lozoya, HE (2019a). A probabilistic approach for seismic risk assessment based on vulnerability
853 functions. Application to Barcelona. Bulletin of Earthquake Engineering, 17(4), 1863-1890.
854 <https://doi.org/10.1007/s10518-018-0516-4>

855 Aguilar-Meléndez A, Pujades LG, de la Puente J, Barbat AH, Ordaz MG, González-Rocha SN, Welsh-
856 Rodríguez CM, Rodríguez-Lozoya HE, Lantada N, Ibarra L, García-Elías A, Campos-Rios A (2019b).
857 Probabilistic assessment of seismic risk of dwelling buildings of Barcelona Implications for the
858 City Resilience. In: Brunetta G, Caldarice O, Tollin N, Rosas-Casals M, Morato J (eds) Urban
859 resilience for risk and adaptation governance: theory and practices. Springer, Dordrecht.
860 https://doi.org/10.1007/978-3-319-76944-8_13

861 Aguilar-Meléndez A, De la Puente J, Monterrubio Velasco M, Rodríguez Lozoya H, Rojas O, Calderón
862 Ramón CM, ... & Campos Rios A (2019c). Analysis of the Key Features of the Seismic Actions Due
863 to the three Main Earthquakes of 11th of May 2011 in Lorca, Spain. Computación y Sistemas,
864 23(2), 365-390.

865 Aguilar-Meléndez A, Ordaz MG, de la Puente J, González Rocha SN, Rodríguez-Lozoya HE, Córdova
866 Ceballos A, García-Elías A, Calderón-Ramón C, Escalante-Martínez JE, Laguna-Camacho JR,
867 Campos- Rios A (2017). Development and validation of software CRISIS to perform probabilistic
868 seismic hazard assessment with emphasis on the recent CRISIS2015. Computación y Sistemas
869 21(1):67–90

870 Aguilar-Meléndez A, Pujades L, Barbat A, Lantada N (2010). A probabilistic model for the seismic risk
871 of buildings: application to assess the seismic risk of buildings in urban areas. A: US National and

- 872 Canadian Conference on Earthquake Engineering. "9th US National and 10th Canadian
873 Conference on Earthquake Engineering". Toronto, p. 1-10.
- 874 Aguilar-Meléndez A, Pujades L, de la Puente J, Barbat A, Lantada N, Campos A (2016). USERISK2015.
875 Program for computing seismic risk in urban areas. <https://sites.google.com/site/userisk2015/>
- 876 Ajuntament de Barcelona (2020). Ciutat Vella. The district and its neighborhoods. Last accessed:
877 2020/07/13 [https://ajuntament.barcelona.cat/ciutatvella/es/el-distrito-y-sus-barrios/el-](https://ajuntament.barcelona.cat/ciutatvella/es/el-distrito-y-sus-barrios/el-distrito-y-sus-barrios)
878 [distrito-y-sus-barrios](https://ajuntament.barcelona.cat/ciutatvella/es/el-distrito-y-sus-barrios/el-distrito-y-sus-barrios)
- 879 Apostol, I, Mosoarca, M, Chieffo, N, & Onescu, E (2019). Seismic vulnerability scenarios for
880 Timisoara, Romania. In Structural Analysis of Historical Constructions (pp. 1191-1200). Springer,
881 Cham. https://doi.org/10.1007/978-3-319-99441-3_128
- 882 Athmani AE, Gouasmia A, Ferreira TM, Vicente R, Khemis A (2015). Seismic vulnerability assessment
883 of historical masonry buildings located in Annaba city (Algeria) using non ad-hoc data survey. Bull
884 Earthquake Eng; 13:2283-2307. <https://doi.org/10.1007/s10518-014-9717-7>
- 885 Barbat AH, Yépez Moya F, Canas JA (1996). Damage scenarios simulation for risk assessment in
886 urban zones, Earthquake Spectra, 2:3, 371-394.
- 887 Barbat AH, Lagomarsino S, Pujades LG (2006). Vulnerability assessment of dwelling buildings. En
888 Oliveira, C. S., Roca, A., Goula, X. (Eds.), Assessing and Managing Earthquake Risk. Dordrecht, pp.
889 115-134. https://link.springer.com/chapter/10.1007/978-1-4020-3608-8_6
- 890 Barbat AH, Pujades LG, Lantada N, Moreno R (2008). "Seismic damage evaluation in urban areas
891 using the capacity spectrum method: application to Barcelona", Soil Dynamics and Earthquake
892 Engineering, 28, 851–865. <https://doi.org/10.1016/j.soildyn.2007.10.006>
- 893 Barbat AH, Carreño ML, Pujades LG, Lantada N, Cardona OD, Marulanda MC (2009). "Seismic
894 vulnerability and risk evaluation methods for urban areas. A review with application to a pilot
895 area", Structure and Infrastructure Engineering, 6(1):17-38.
896 <https://doi.org/10.1080/15732470802663763>
- 897 Basset-Salom, L, & Guardiola-Villora, A (2020). Seismic Vulnerability and Expected Damage in
898 "Ground Zero Area" in El Cabanyal (Valencia). International Journal of Architectural Heritage, 1-
899 18. <https://doi.org/10.1080/15583058.2019.1710783>
- 900 Bernardini, A, Giovinazzi, S, Lagomarsino, S, Parodi, S (2007a). The vulnerability assessment of
901 current buildings by a macroseismic approach derived from the EMS-98 scale. Memorias del 3er
902 Congreso Nacional de Ingeniería Sísmica, Girona, Cataluña, mayo, 15 pp.
- 903 Bernardini A, Giovinazzi S, Lagomarsino S, Parodi S (2007b). Matrici di probabilità di danno implicite
904 nella scala EMS-98. Pisa, Italy: 12th Italian Conference on Earthquake Engineering, June.
- 905 Carreño ML, Cardona OD, Barbat AH (2007). "Urban seismic risk evaluation: A ho-listic approach",
906 Natural Hazards, 40, 137-172. <https://doi.org/10.1007/s11069-006-0008-8>
- 907 Cherif SE, Chourak M, Abed M, Pujades L (2016). Seismic risk in the city of Al Ho-ceima (north of
908 Morocco) using the vulnerability index method, applied in Risk-UE project. Natural Hazards, 1-
909 19. <https://doi.org/10.1007/s11069-016-2566-8>
- 910 Cid, J, Figueras, S, Fleta, J, Goula, X, Susagna, T, Amieiro, C (1999). Zonación Sísmica de la Ciudad de
911 Barcelona. Primer Congreso Nacional de Ingeniería Sísmica, Murcia, España, pp. 263-271.

912 Dolce M, Kappos A, Masi A, Penelis G, Vona M (2006). Vulnerability assessment and earthquake
913 damage scenarios of the building stock of Potenza (Southern Italy) using Italian and Greek
914 methodologies, *Engineering Structures*, 28: 357-371.

915 Faccioli, E, Frassinè, L, Finazzi, D, Pessina, V, Cauzzi, C, Lagomarsino, S, Giovinazzi, S, Resemini, S,
916 Curti, E, Podestà, S, Scuderi, S (2004). Synthesis of the application to Catania city. RISK-UE. An
917 advanced approach to earthquake risk scenarios with applications to different European towns.
918 Contract: EVK4-CT-2000-00014.

919 Ferreira, TM, Vicente, R, Mendes da Silva, JAR et al. (2013). Seismic vulnerability assessment of
920 historical urban centres: case study of the old city centre in Seixal, Portugal. *Bull Earthquake Eng*
921 11, 1753–1773. <https://doi.org/10.1007/s10518-013-9447-2>

922 Ferreira, TM, Maio, R, Costa, AA, & Vicente, R (2017a). Seismic vulnerability assessment of stone
923 masonry façade walls: Calibration using fragility-based results and observed damage. *Soil*
924 *Dynamics and Earthquake Engineering*, 103, 21-37.
925 <https://doi.org/10.1016/j.soildyn.2017.09.006>

926 Ferreira, TM, Maio, R, & Vicente, R (2017b). Seismic vulnerability assessment of the old city centre
927 of Horta, Azores: calibration and application of a seismic vulnerability index method. *Bulletin of*
928 *Earthquake Engineering*, 15(7), 2879-2899. <https://doi.org/10.1007/s10518-016-0071-9>

929 Giovinazzi S (2005). The vulnerability assessment and the damage scenario in seismic risk analysis.
930 Doctoral thesis, Technical University of Braunschweig, and University of Florence, 222 pp.

931 Giuliani, F, De Falco, A, Sevieri, G, & Cutini, V (2019). Managing emergency into historic centres in
932 Italy: seismic vulnerability evaluation at urban scale. In *COMPDYN Proceedings (Vol. 1, pp. 1641-*
933 *1652)*. European Community on Computational Methods in Applied Sciences (ECCOMAS).

934 Goula, X, Susagna, T, Secanell, R, Fleta, J, Roca, A (1997). Seismic Hazard Assessment for Catalonia
935 (Spain). *Proceedings Second Congress on Regional Geological Cartography and Information*
936 *Systems*, Barcelona, pp.173-177.

937 Guardiola-Víllora A, Basset-Salom L (2015). Escenarios de riesgo sísmico del distrito del Eixample de
938 la ciudad de Valencia. *Revista Internacional de Métodos Numéricos para Cálculo y Diseño en*
939 *Ingeniería*, 31(2), 81-90. <http://dx.doi.org/10.1016/j.rimni.2014.01.002>

940 Guardiola-Víllora A, & Basset-Salom L (2020). Earthquake risk scenarios of the Ciutat Vella District
941 in Valencia, Spain. *Bulletin of earthquake engineering*, 18(4), 1245-1284.
942 <https://doi.org/10.1007/s10518-019-00745-7>

943 Hardy, G, Richards, J, Kassawara, R, & Mauer, A (2017). US nuclear power industry seismic
944 mitigation strategy assessment (msa) approach. 24th Conference on Structural Mechanics in
945 Reactor Technology. BEXCO, Busan, Korea - August 20-25.

946 Idescat (2021a). Barcelona. The municipality in figures. Statistical Institute of Catalonia.
947 <https://www.idescat.cat/emex/?id=080193&lang=en> Accessed 10 July 2021

948 Idescat (2021b). Barcelona. Distribution by districts. 2020.
949 <https://www.idescat.cat/poblacioestrangera/?b=10&geo=mun:080193&lang=en> Accessed 10
950 July 2021

951 IGN (2017). Actualización de mapas de peligrosidad sísmica de España 2012. Instituto Geográfico
952 Nacional. Centro Nacional de Información Geográfica. <https://doi.org/10.7419/162.05.2017>

953 Irizarry, J (2004). An Advanced Approach to Seismic Risk Assessment. Application to the Cultural

954 Heritage and the Urban system of Barcelona. Doctoral thesis, Universitat Politècnica de
955 Catalunya, Barcelona, 406 pp.

956 Irizarry J, Lantada N, Pujades LG, Barbat AH, Goula X, Susagna T, Roca A (2011). Ground-shaking
957 scenarios and urban risk evaluation of Barcelona using the Risk-UE capacity spectrum based
958 method; *Bulletin of Earthquake Engineering* (9)2: 441-466. <https://doi.org/10.1007/s10518-010-9222-6>
959

960 Kassem, MM, Nazri, FM, & Farsangi, EN (2020). The seismic vulnerability assessment methodologies:
961 A state-of-the-art review. *Ain Shams Engineering Journal*, 11(4), 849-864.
962 <https://doi.org/10.1016/j.asej.2020.04.001>

963 Lagomarsino S, & Giovinazzi S (2006). Macroseismic and mechanical models for the vulnerability
964 and damage assessment of current buildings. *Bulletin of Earthquake Engineering*, 4(4), 415-443.
965 <https://doi.org/10.1007/s10518-006-9024-z>

966 Lantada N (2007). Evaluación del riesgo sísmico mediante métodos avanzados y técnicas GIS.
967 Aplicación a la ciudad de Barcelona. Tesis doctoral, Vol. 1., Universitat Politècnica de Catalunya,
968 Barcelona, 338 pp.

969 Lantada N, Pujades LG, Barbat AH (2009). "Vulnerability index and capacity spectrum based methods
970 for urban seismic risk evaluation. A comparison", *Natural Hazards*, 51:501-524.
971 <https://doi.org/10.1007/s11069-007-9212-4>

972 Lantada N, Irizarry J, Barbat AH, Goula X, Roca A, Susagna T, Pujades LG (2010). Seismic hazard and
973 risk scenarios for Barcelona, Spain, using the Risk-UE vulnerability index method. *Bulletin of*
974 *earthquake engineering*, 8(2), 201-229. <https://doi.org/10.1007/s10518-009-9148-z>

975 Lantada N, Pujades LG, Barbat AH (2018). Earthquake risk scenarios in urban areas: a review with
976 applications to the Ciutat Vella district in Barcelona, Spain. *International Journal of Architectural*
977 *Heritage*, 12(7-8), 1112-1130. <https://doi.org/10.1080/15583058.2018.1503367>

978 Lestuzzi P, Podestà S, Luchini C, Garofano A, Kazantzidou-Firtinidou D, Bozzano C, ... & Rouiller JD
979 (2016). Seismic vulnerability assessment at urban scale for two typical Swiss cities using Risk-UE
980 methodology. *Natural Hazards*, 1-21. <https://doi.org/10.1007/s11069-016-2420-z>

981 López-Casado C, Molina S, Delgado J, Peláez JA (2000). Attenuation of intensity with epicentral
982 distance in the Iberian Peninsula. *Bull Seismol Soc Am* 90:34-47

983 Maio, R, Ferreira, TM, Vicente, R, & Estêvão, J (2016). Seismic vulnerability assessment of historical
984 urban centres: Case study of the old city centre of Faro, Portugal. *Journal of Risk Research*, 19(5),
985 551-580. <https://doi.org/10.1080/13669877.2014.988285>

986 Marulanda MC, Carreño ML, Cardona OD, Ordaz MG, Barbat AH (2013). Probabilistic earthquake
987 risk assessment using CAPRA: application to the city of Barcelona, Spain. *Natural hazards*, 69(1),
988 59-84. <https://doi.org/10.1007/s11069-013-0685-z>

989 Mezcuca J, Rueda J, & Blanco RMG (2020). Characteristics of a new regional seismic-intensity
990 prediction equation for Spain. *Natural Hazards*, 1-16. <https://doi.org/10.1007/s11069-020-03897-x>
991

992 Milutinovic ZV, Trendafiloski GS (2003). WP4: Vulnerability of current buildings. RISK-UE. An
993 advanced approach to earthquake risk scenarios with applications to different Euro-pean towns,
994 Contract: EVK4-CT-2000-00014, 109 pp.

- 995 Neves, F, Costa, A, Vicente, R, Oliveira, CS, & Varum, H (2012). Seismic vulnerability assessment and
 996 characterisation of the buildings on Faial Island, Azores. *Bulletin of Earthquake Engineering*,
 997 10(1), 27-44. <https://doi.org/10.1007/s10518-011-9276-0>
- 998 Ojeda, A, Atakan, K, Masana, E, Santanach, P, Jiménez, MJ, García Fernández, M (2002). Integration
 999 and influence of paleoseismic and geologic data for the seismic hazard evaluation in the Catalan
 1000 coastal ranges, Spain; *Soil Dynamics and Earthquake engineering* 22: 911-916.
 1001 [https://doi.org/10.1016/S0267-7261\(02\)00114-8](https://doi.org/10.1016/S0267-7261(02)00114-8)
- 1002 Ordaz M, Martinelli F, Aguilar-Meléndez A, Arboleda J, Meletti C, D'Amico V (2015). CRISIS2015.
 1003 Program for computing seismic hazard. <https://sites.google.com/site/codecrisis2015/>. Accessed
 1004 15 May 2020
- 1005 Ordaz M, Martinelli F, Aguilar-Meléndez A, Arboleda J, Meletti C, D'Amico V (2020). R-CRISIS.
 1006 Program for computing seismic hazard. Last accessed: 2020/05/18. <http://www.r-crisis.com/>
- 1007 Ortega, J, Vasconcelos, G, Rodrigues, H, & Correia, M (2019). A vulnerability index formulation for
 1008 the seismic vulnerability assessment of vernacular architecture. *Engineering Structures*, 197,
 1009 109381. <https://doi.org/10.1016/j.engstruct.2019.109381>
- 1010 Pujades LG, Canas JA, Mena U, Espinoza F, Alfaro A, Caselles J (2000). Seismic Risk Evaluation in
 1011 Barcelona, Spain. *Proceedings of the 12th World Conference on Earthquake Engineering*, Auckland,
 1012 New Zealand, pp.8.
- 1013 Pujades LG, Barbat AH, Lantada N (2007). Evaluación del riesgo sísmico en zonas urbanas: desarrollo
 1014 de escenarios. *Revista internacional de ingeniería de estructuras*; 12(1): 1-28.
- 1015 Romis, F, Caprili, S, Salvatore, W, Ferreira, TM, & Lourenço, PB (2020). Seismic vulnerability
 1016 assessment of historical urban centres: The case study of campi alto di norcia, Italy. *The*
 1017 *International Archives of Photogrammetry, Remote Sensing and Spatial Information Sciences*,
 1018 44, 885-892.
- 1019 Ruiz A, Vidal-Sanchez F, Aranda-Caballero C (2015). Estudio de la Vulnerabilidad Sísmica del Centro
 1020 Histórico de Tapachula, Chiapas, con el Método del Índice de Vulnerabilidad. *Revista*
 1021 *Internacional Desastres Naturales, Accidentes e Infraestructura Civil*. 15(1), 5-24.
- 1022 Secanell, R, Goula, X, Susagna, T, Fleta, J, Roca, A (2004). Seismic hazard zonation of Catalonia, Spain,
 1023 integrating random uncertainties, *Journal of Seismology*, 8:25-40.
- 1024 Solomos, G, Pinto, A, & Dimova, S (2008). A review of the seismic hazard zonation in national
 1025 building codes in the context of eurocode 8. *JRC Scientific and Technical reports*.
- 1026 Stirrat, AT, & Jury, RD (2017). Performance versus Compliance of Buildings in the Seismic Context.
 1027 In *New Zealand Society for Earthquake Engineering Annual Conference*.
- 1028 Taibi, H, Ait Youcef, M & Khellafi, M (2020). Seismic vulnerability assessment using the macroseismic
 1029 method proposed in the framework of Risk-UE project based on the recommendations of the
 1030 Algerian seismic code RPA99/Version 2003. *Asian J Civ Eng* 21, 59–66.
 1031 <https://doi.org/10.1007/s42107-019-00190-6>
- 1032 UNISDR (2015). Sendai framework for disaster risk reduction 2015–2030.
 1033 https://www.unisdr.org/files/43291_sendaiframeworkfordrren.pdf. Accessed 11 May 2020
- 1034 Vacareanu, R, Lungu, D, Aldea, A, Arion, C (2004). WP7: Seismic Risk Scenarios Handbook. RISK-UE.
 1035 An advanced approach to earthquake risk scenarios with applications to different European
 1036 towns, Contract: EVK4-CT-2000-00014, 51 pp.

1037 Vicente, R, Parodi, S, Lagomarsino, S et al. (2011). Seismic vulnerability and risk assessment: case
1038 study of the historic city centre of Coimbra, Portugal. Bull Earthquake Eng 9, 1067–1096.
1039 <https://doi.org/10.1007/s10518-010-9233-3>